Universidade de Lisboa

Faculdade de Ciências

Departamento de Biologia Animal

Hox-code in Thymus Identity

Ana Sofia Salvador Santos

Dissertação

Mestrado em Biologia Evolutiva e do Desenvolvimento

2013

Universidade de Lisboa

Faculdade de Ciências

Departamento de Biologia Animal

Hox-code in Thymus Identity

Ana Sofia Salvador Santos

Dissertação

Mestrado em Biologia Evolutiva e do Desenvolvimento

Orientadores

Professora Dra. Rita Maria Pulido Garcia Zilhão (DBV/FCUL)

Professora Dra. Hélia Cristina de Oliveira Neves (IHBD/FMUL)

2013

Acknowledgments

Chegado o final desta etapa, é preciso relembrar e agradecer as todas as pessoas que participaram e tornaram possível a concretização deste projecto e desta fase da minha vida.

Hélia, quero em primeiro lugar agradecer-lhe, pois sem si, nada teria sido possível. Aceitou-me como sua aluna para este projecto de Mestrado e acreditou no meu potencial para realizá-lo. Neste último ano fez-me crescer tanto a nível profissional como a nível pessoal. Obrigada pela sua dedicação, confiança e paciência, por tudo o que me ensinou e especialmente por me ter aberto as portas à investigação.

Prof. Rita, quero agradecer-lhe também por todo o apoio que me deu ao longo deste ano. Tal como a Hélia, acreditou no meu potencial e ajudou-me e acompanhou-me em muitas fases deste projecto. Obrigada por todo o conhecimento que partilhou comigo durante este ano e pela paciência, dedicação e motivação que me ofereceu.

Marta e Joana, tenho muito por que vos agradecer. Sem vocês, este ano e a realização deste projecto não teriam sido os mesmos. Foi um ano de muito trabalho mas também de muitas conversas, risos, partilhas e brincadeiras. Obrigada por todo o apoio! Espero um dia conseguir retribuir toda a ajuda e disponibilidade que ofereceram. Foram mais do que colegas, foram companheiras e amigas e marcaram de uma forma muito positiva este trabalho e este ano.

Quero agradecer também aos restantes elementos da Unidade de Células Estaminais e Organogénese, especialmente à Isabel e ao Vítor. A vossa dedicação e disponibilidade foram essenciais para a finalização deste trabalho.

Deixo também um agradecimento especial à Raquel Andrade, por nos ter cedido as sondas que foram essenciais para a realização deste trabalho.

Família e amigos, agradeço-vos pela vossa força e o vosso carinho. Especialmente:

À Samanta, por tudo o que temos partilhado nos últimos anos. Estás sempre presente, nos bons e nos maus momentos, sempre com uma palavra amiga, um conselho, um sorriso. Obrigada por toda a força e preocupação, particularmente nas últimas semanas.

Ao Daniel, que nos últimos 5 anos, para além de Arquitectura tem-se "especializado" em Biologia. Obrigada por estares sempre do meu lado, por me acompanhares em todas as fases, dando-me sempre força para nunca desistir. Na fase final deste projecto, foste incansável e ajudaste-me em tudo o que te era possível. Obrigada pela dedicação, pelo carinho e pela paciência.

Aos meus pais. Tudo o que sou e consegui até hoje, devo-vos a vocês. Obrigada pelo vosso amor, carinho, compreensão, empenho, preocupação e dedicação, que me fizeram sentir segura e confiante em todas as fases da minha vida e em todas as pequenas conquistas.

Abstract

In jaw vertebrates, thymus is a primary hematopoietic organ responsible for T-cell differentiation. The thymus derives from the endoderm of the 3rd and 4th pharyngeal pouches (3/4 PP) in avian. However, in distinct species, the thymus can derive from other PP. Such anterior-posterior (AP) diversity of thymus positional origin has become of great interest to evolutionary developmental biology.

The transcription factors Homeobox (Hox) genes are responsible for positional identity during development and are ruled out by a spatially collinear of gene expression along the AP-axis of the embryo and by phenotypic suppression by posterior genes.

In this study we aimed to identify a potential Hox-code responsible for the positional identity of the thymus. For that, we first characterized the expression pattern of Hox-genes in the pharyngeal region of chick embryos, by whole-mount *in situ* hybridization, at stages prior to thymus formation. We observed that PP positional identity could be defined by an orderly expression of *Hox* genes with *HoxA3* and *HoxB1* defining the anterior frontiers of the 3 PP and 4PP, respectively. We hypothesised that *HoxA3* and *HoxB1* may be the potential Hox-code responsible for positional identity of thymic rudiment.

To test our hypothesis we intend to ectopically express *HoxA3* and *HoxB1*, in the 2PP and 3PP respectively. To genetically modify the PP endoderm, we already produced a pT2K-HoxA3eGFP construct to be used in the combined system of vectors, “Tol2-mediated gene transfer” and “Tetracycline-dependent conditional expression”. To test the efficiency of this system of vectors we transfected the HEK 293T cell line with the control-vectors and we monitored its efficacy by fluorescence microscopic observation and flow cytometry analysis. Long-term culture of transfected cells showed modest genomic integration of these vectors and “leakage” of the system when modulated by doxycycline.

Keywords: thymus positional identity, pharyngeal pouch identity, endoderm, Hox-code, *HoxA3*, *HoxB1*

Resumo

Em vertebrados que apresentam mandíbula, o timo é um órgão especializado do sistema imunitário adaptativo e o principal órgão hematopoiético responsável pela produção e diferenciação de células-T "auto-restritas" e "auto-tolerantes". A produção destas células-T está dependente da interação entre as suas células percursoras, os timócitos, e as células epiteliais tímicas (CET), células especializadas do nicho tímico.

O desenvolvimento do timo é acompanhado pelo desenvolvimento das glândulas paratiróides, pois partilham a mesma origem embrionária, as bolsas faríngicas (BF). Em galinha, foi demonstrado que os domínios presuntivos do timo e das glândulas paratiróides são identificados na endoderme da 3ª e 4ª BF pela expressão dos factores de transcrição *Foxn1* e *Gcm2*, respectivamente.

No entanto, entre as diferentes espécies de vertebrados, o timo pode derivar de diferentes bolsas faríngicas. Nos peixes cartilagíneos, considerados o grupo de espécies mais primitivo a desenvolver timo, como por exemplo o tubarão, o timo deriva conjuntamente das 2ª à 6ª BF. No caso dos anfíbios, a origem do timo é a 2ª BF e nos répteis desenvolve-se a partir da 2ª e da 3ª BF. Em aves, o timo deriva das 3ª e 4ª BF e nos mamíferos apenas da 3ª BF.

A extraordinária diversidade, ao longo do eixo anterior-posterior (A-P), no número de BF com potencial para o desenvolvimento do timo tornou-se uma questão de grande interesse para a biologia evolutiva e do desenvolvimento e remete para o estudo de mecanismos moleculares conservados evolutivamente, que ocorrem em estadios precoces do desenvolvimento das BF, nomeadamente da 3ª e da 4ª bolsas.

Os genes Homeobox (Hox) são factores de transcrição, evolutivamente conservados entre filos e são os genes responsáveis pela especificação do plano corporal, nomeadamente do eixo A-P. Estes genes por sua vez, são governados pelas regras da colinearidade espacial da sua expressão génica ao longo do eixo A-P do embrião e pela prevalência posterior ou supressão fenotípica dos genes posteriores. Diferentes estudos sobre o padrão de expressão dos genes Hox em ratinho e galinha sugerem a existência de um código formado por combinações específicas destes genes que determinam uma região específica do eixo A-P do embrião. De um ponto de vista evolutivo, a existência de um código-Hox a nível das BF, conservado entre vertebrados, poderia explicar a diversidade no número de BF com potencial para o desenvolvimento do timo.

Múltiplos estudos em ratinho e galinha demonstraram o papel fundamental de *HoxA3* na formação do 3º arco e 3ª bolsa faríngicos e nos seus derivados. Surpreendentemente, o fenótipo da mutação *HoxA3* em ratinho é muito semelhante ao fenótipo apresentado por doentes com síndrome de DiGeorge: não apresentam timo nem glândulas paratiróides, apresentam hipoplasia da tiroide e múltiplos defeitos na estrutura dos 3º e 4º arcos faríngicos. Estas evidências sugerem um importante papel deste gene na identidade da bolsa de origem do timo e possivelmente na própria identidade posicional do timo.

Neste projecto, o nosso príncipal objectivo foi a identificação de um possível código Hox responsável pela identidade posicional do timo na 3ª e 4ª BF no embrião de galinha. Para tal e

com o objectivo de identificar quais os genes Hox expressos na endoderme da 3ª e 4ª BF, começamos por realizar hibridações *in situ* em embriões de galinha nos estadios E3 e E4, estadios anteriores à formação do timo. Foram caracterizados os padrões de expressão dos genes *HoxA2*, *HoxA3*, *HoxB1*, *HoxB2*, *HoxB3* e *HoxB4*, alguns dos genes Hox expressos mais anteriormente no embrião. De forma a obtermos informação mais detalhada da expressão destes genes nos tecidos mais internos da região faríngica, os embriões foram processados pós-hibridação para cortes histológicos. Neste estudo foram também desenvolvidas novas sondas para os genes *HoxA3*, *HoxB2* e *HoxB4*. A análise dos padrões de expressão génica na região faríngica revelou a expressão ordenada de genes HoxA ao longo do eixo A-P. Nomeadamente, observámos a expressão de *HoxA2* a partir do 2º arco faríngico (AF) e especificamente na 2ª BF e expressão de *HoxA3* a partir do 3º AF e especificamente na 3ª BF. Relativamente à expressão dos genes do grupo HoxB, não se observou uma expressão padronizada ao longo do eixo A-P. O padrão de expressão de *HoxB1* foi observado unicamente na porção posterior da endoderme da 4ª BF. No caso dos genes *HoxB2*, *HoxB3* e *HoxB4,* a sua expressão foi observada no mesênquima da região posterior à 4ª BF. Curiosamente, também foi observada expressão de *HoxB4* ao nível da porção posterior da endoderme da 4ª BF. Estes resultados sugerem que a identidade posicional das diferentes BF pode ser definida por uma combinação específica de genes Hox. Em particular, sugerem que os genes *HoxA3*, *HoxB1* e *HoxB4* se encontram a definir as fronteiras anteriores da 3ª e 4ª BF. No entanto, estudos em ratinho demonstraram que *HoxB4* está apenas envolvido na especificação da região ventral do embrião, sugerindo que este não está envolvido na identidade posicional das BF. Com estes resultados, levantamos assim a hipótese da combinação $HoxA3^{+}HoxB1^{-}$ ser o código responsável pela identidade posicional do timo.

Para testar esta hipótese, desenhámos um ensaio funcional *in vivo* em que a endoderme de diferentes BF é modificada geneticamente para expressar de forma ectópica os genes Hox. Especificamente, o nosso objectivo era sobre-expressar HoxA3 e HoxB1, na 2ª BF e 3ª BF, respectivamente, por forma a modificar a identidade posicional das mesmas. Para modificar geneticamente a endoderme, utilizamos um sistema de vectores que combina a "Transferência génica mediada por *Tol2*" e a "expressão condicional dependente de tetraciclina" (desenvolvido por Y. Takahashi e colaboradores).

Para a utilização deste sistema no nosso trabalho, foram desenhados 2 novos vectores: pT2K-HoxA3eGFP, para a expressão de *HoxA3* e pT2K-HoxB1eGFP para a expressão de *HoxB1*. Durante a realização desta tese, realizámos a construção do primeiro vector, encontrando-se o segundo em construção. Para testar a eficiência do sistema de vectores utilizamos uma linha celular humana, a linha HEK 293T. Esta foi transfectada com o sistema de vectores (controlo), em condições que permitissem avaliar a capacidade de integração genómica e a resposta deste sistema quando modulado por doxiciclina (doxy). A cultura de células transfectadas foi avaliada por observação ao microscópio de fluorescência e analisada por citometria de fluxo. Os resultados obtidos, ao longo de 14 dias, demonstraram uma rápida e drástica redução tanto na percentagem de células a expressar GFP como na intensidade média de fluorescência de GFP, sugerindo uma reduzida capacidade de integração dos vectores deste sistema no genoma. Para avaliar a resposta do sistema quando modulado pela presença/ausência de doxy, as células foram transfectadas na presença de doxy. Células transfectadas e cultivadas na presença de doxy apresentaram, aproximadamente, 20% de células GFP^{+} após 48h de cultura.

Este resultado demostrou que este sistema não bloqueia eficientemente a expressão de GFP, sugerindo a existência de um "*leakage*" na modulação pela doxy. No entanto, foi observado, que a presença continuada de doxy levou à redução da intensidade média de fluorescência das células GFP^+, após 10-14 dias em cultura, sugerindo que este "*leakage*" é responsável por níveis muito baixos de expressão génica. Foi também observado, que a remoção de doxy às 48h de cultura levou a um aumento da intensidade média de fluorescência das células GFP^+. Estes dados sugerem que este sistema de vectores é modulado negativamente pela doxy, pois na sua presença, o sistema bloqueia a expressão de GFP.

De futuro, com as construções de vectores finalizadas e as condições de utilização do sistema de vectores aferidas, iremos realizar os ensaios funcionais que permitam avaliar a possível mudança de identidade das bolsas por expressão ectópica dos genes *HoxA3* e *HoxB1* nas 2ª e 3ª BF, respectivamente. Resumidamente, as endodermes isoladas da 2ª e da 3ª BF serão geneticamente modificadas com os plasmídeos pT2K-HoxA3eGFP e pT2K-HoxB1eGFP (neste sistema de vectores), respectivamente. Serão depois cultivadas *in vitro* com mesênquima permissivo e posteriormente enxertadas na membrana corioalantóide para testar a formação dum timo (desenvolvimento *in ovo*). Com este ensaio esperamos mostrar o "ganho-de-potencialidade" da 2ª BF e a "perda-de-potencialidade" da 3ª BF, na formação do timo. A conjugação deste sistema de vectores com o ensaio funcional oferece uma abordagem experimental única para a identificação dum putativo código-Hox responsável pela identidade posicional do timo.

Palavras-chave: identidade posicional do timo, identidade das bolsas faríngicas, endoderme, código-Hox, *HoxA3*, *HoxB1*

Index

Abbreviations

bp – base pairs
d, h, m, sec – day, hour, minute, second
doxy – Doxycycline
DMEM – Dulbecco's Modified Eagle Medium
DNA – Deoxyribonucleic Acid
E – Embryonic day
EDTA – Ethylenediaminetetraacetic Acid
FBS – Fetal Bovine Serum
GFP – Green Fluorescence Protein
GFP^+– GFP positive
MFI – median fluorescence intensity
ng/mL – nanogram per milliliter
o/n – overnight
PA – Pharyngeal Arch
PBS – Phosphate Buffered Saline
Pen/Strep – Penicillin/Streptomycin
PFA – Paraformaldehyde
PP – Pharyngeal Pouch
RNA – Ribonucleic Acid
rpm – Revolutions per minute
PCR –Polymerase Chain Reaction
U/µL – units per microliter
µg/mL – microgram per milliliter
v/v – volume/volume

I. Introduction

I.1. Development of the pharyngeal region in vertebrates

During vertebrate embryogenesis, the pharyngeal apparatus develops from a transient series of segmental structures, appearing as bulges on the cranial lateral side of the embryo, named Pharyngeal Arches (PA). Between adjacent arches, the pharynx endoderm evaginates laterally forming the pharyngeal pouches (PP). Externally, the ectoderm depresses forming the pharyngeal cleft. The PA comprise tissues derived from the 3 germ layers: externally the arch is composed by ectoderm, inner covered by endoderm and its core is thought to be composed of mesoderm surrounded by neural crest cells (NCCs). Each of these different embryonic populations will generate distinct derivatives (Figure 1): the NC will develop into cartilage, connective tissues and smooth muscle; the mesoderm, musculature and endothelial cells; the ectoderm will form the epidermis and neurogenic placodes; the endoderm will give rise to the epithelium, taste buds, thyroid, thymus and pharathyroid glands (Graham & Smith, 2001; Graham, 2001; Graham & Richardson, 2012; Grevellec & Tucker, 2010).

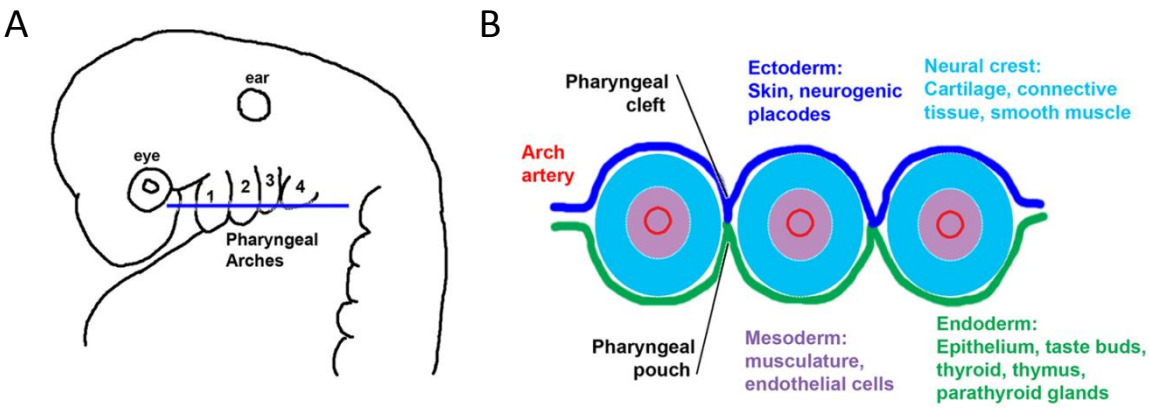

Figure 1| Schematic representation of the pharyngeal apparatus. (A) Lateral view of an amniote embryo, with pharyngeal arches identified from 1-4 in an anterior to posterior manner. **(B)** Transverse section through the arch region represented in (A), showing the constituent tissues: ectoderm, dark blue; endoderm, green; neural crest, pale blue ; mesoderm, purple. [adapted from Graham & Richardson, 2012]

Although these structures are found in all vertebrates, it appears to be a trend towards the loss on the number of PA, reflecting the alteration in function of the different pharyngeal structures. For instances, shifting from filter feeding to a predatory behavior, which led to the appearance of the jaw. Also, in aquatic to terrestrial transition, during tetrapods' evolution, the necessity for regulation of calcium and phosphorous led to the appearance of the parathyroid gland and the shift to lungs as the major respiratory organs. Therefore, caudal arches no longer had to support gills. This trend has been associated to the role of endoderm as the major organizer of the pharyngeal region development, and not the neural crest (Graham & Richardson, 2012; Grevellec & Tucker, 2010). Different developmental studies have shown that ablation of the neural crest does not prevent initial formation PP, suggesting it is

independent from the migrating crest (Veitch, Begbie, Schilling, Smith, & Graham, 1999). Also, Couly and colleagues demonstrated that removal of the foregut endoderm in the chick led to failure in development of the pharyngeal skeleton and ectopic grafts of foregut endoderm led to duplication of skeleton elements (Couly, Creuzet, Bennaceur, Vincent, & Le Douarin, 2002).

The different PA and PP generate specific tissues and organs. For this project I'm going to focus in the formation of the thymus and the parathyroid glands, organs derived from the 3rd and 4th PP (3/4PP), in birds and mammals.

I.2. The thymus and parathyroid glands development

As a specialized organ of the adaptative immune system, the thymus is the primary site for T-lymphocytes (T-cell) development. The thymus is a capsulated epithelial organ, histological divided into two compartments, cortex and medulla containing distinct thymic epithelial cells (TECs) subtypes. This thymic architecture provides a unique environment for thymocytes (developing T-cells) differentiation. The parathyroids are endocrine glands responsible for the production of the parathyroid hormone (PTH), a peptidic hormone essential to regulate calcium and phosphate homeostasis (Julie Gordon & Manley, 2011; Grevellec & Tucker, 2010).

Thymus and parathyroid glands have the same embryological origin: the endoderm of the PP (3/4PP chicken, 3PP in mammals), previously demonstrated (Blackburn & Manley, 2004; Cordier & Haumont, 1980; L. Douarin & Jotereau, 1975; Farley et al., 2013).

The expression domains of two transcription factors, *Foxn1* (forkhead box N1) and *Gcm2* (glial cells missing-2), were shown to identify the rudiments of the thymus and parathyroid glands in the pouches, respectively (Gordon, Bennett, Blackburn, & Manley, 2001). In mouse and human, thymic and parathyroid rudiments are located ventrally and dorsal-proximally in the 3PP, respectively (Farley et al., 2013; Gordon et al., 2001). Foxn1 is required cell-autonomously for thymic epithelium differentiation and LPC colonization. Loss-of function of *Foxn1* in nude mice led to athymia, as LPCs fails to enter the primordium and remains in surrounding mesenchyme and the epithelial cells fail to expand within the primordium (Blackburn et al., 1996; Bleul et al., 2006; Gordon et al., 2001; Nehls et al., 1996). Deletion of Gcm2 marker leads to no formation of the parathyroid glands, with no interference in thymus development (Günther et al., 2000; Liu et al., 2007).

In chicken, transcription factors *Foxn1* and *Gcm2* were expressed in the prospective domains of the thymus and parathyroid glands, respectively. *Foxn1* expression was identified in the thymus rudiment, in the most dorsal region of the 3/4 PP endoderm in chicken embryo at E4.5 (Figure 2A and C). *Gcm2* expression, preceding the parathyroid glands rudiment, was identified ventral/anterior region of the 3/4 PP (Figure 2B and C) (Neves, Dupin, Parreira, & L. Douarin, 2012).

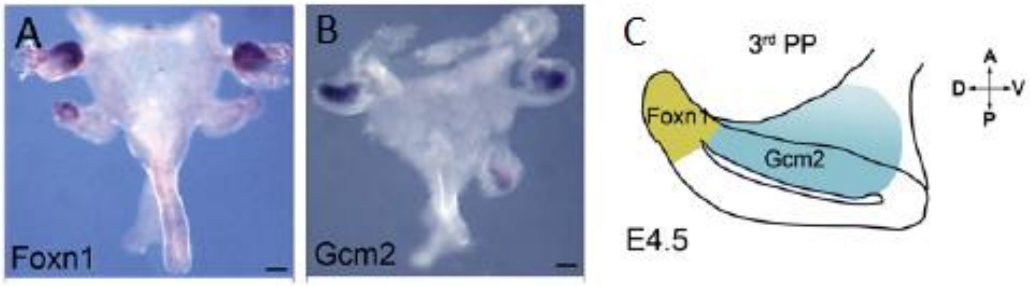

Figure 2|Expression of *Foxn1* and *Gcm2* during thymic and parathyroid glands development in chick embryos. *In situ* hybridization showing *Foxn1 (A)* and *Gcm2 (B)* expression in the isolated 3/4 PP endoderm of E4.5 chicken embryos. Schematic representation of the expression domains of *Foxn1* and *Gcm2* in the 3PP endoderm of E4.5 chicken embryos (C). A, anterior; D, dorsal; P, posterior; PP, pharyngeal pouch; V, ventral. [adapted from Neves *et al.*, 2012]

Thymus organogenesis is a dynamic process that occurs in two main phases: a thymocyte-independent phase followed by a thymocyte-dependent. In the first one, the endoderm and the surrounding mesenchyme (NC-derived) interact to direct TECs specification (Gordon & Manley, 2011; Rodewald, 2008). In the second phase, thymic anlage is dependent of lymphoid progenitor cells (LPCs) colonization which allows the maturation of the thymic epithelium into cortical (cTECs) and medullar (mTECs) compartments (Alves, Huntington, Rodewald, & Di Santo, 2009; Blackburn & Manley, 2004; Gordon & Manley, 2011; Rodewald, 2008).

Using the quail-chick chimera system, Le Douarin and colleagues showed that epithelial-mesenchymal interactions are essential in early – phase of thymic development. Furthermore, they showed that heterologous mesenchymal tissues (derived from the somatopleure or splanchnopleure) have the ability to mimic the role of neural crest-derived mesenchyme. Briefly, quail 3/4 PP endoderm grafted into heterologous mesenchyme from a chick at embryonic day 3 (E3) was able to develop into thymic epithelium. Moreover, the endoderm appeared to be capable of inducing the heterologous mesenchyme to participate in the formation of a fully developed thymus. Therefore, this mesenchyme was considered "permissive" to endoderm development (L. Douarin & Jotereau, 1975; L. Douarin, 1967).

H. Neves and colleagues working on the thymocyte-independent stage of thymus organogenesis, unraveled some of the early molecular events occurring during this developmental window (Neves et al., 2012). Taking advantage of quail-chick chimeras, they demonstrated that cellular interactions between the endoderm and surrounding mesenchyme involved a sequential mesenchymal-derived expression of *Bmp4* and *Fgf10*, essential for the development of the 3/4 PP endoderm into thymic and parathyroid glands epithelial. It was also observed a temporal regulation of *Bmp4* expression in the mesenchymal compartment, suggesting Bmp4 levels to be tightly regulated in the developing pouches. It was proposed a model (see Figure 3) for the crosstalk between Bmp and Fgf signaling molecules during tissue interaction in thymic and parathyroid development, emphasizing the highly dynamic temporal and spatial dialogue between the PP endoderm and mesenchyme. Nevertheless, the signals from the early 3/4PP endoderm, which can induce the mesenchyme to participate in thymus and parathyroid glands development remain to be identified (Neves et al., 2012).

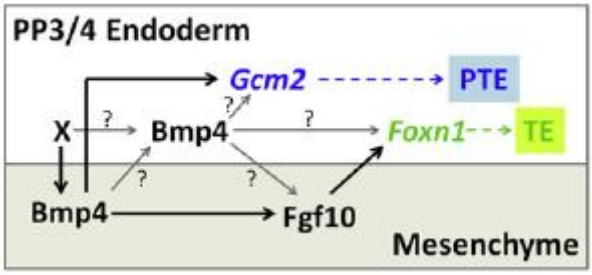

Figure 3 | Schematic model of Bmp and Fgf signaling crosstalk during epithelial-mesenchymal interactions in early thymic and parathyroid development. A highly dynamic temporal and spatial dialogue occurs between the 3/4 PP endoderm and surrounding mesenchyme, in which signals from the endoderm induce the mesenchyme to participate in thymus and parathyroid glands formation. Arrows indicate putative signalling crosstalk involved in the epithelial-mesenchymal dialogue. [adapted from Neves *et al.*, 2012]

Among vertebrate, the thymus is only present in jawed species and it can be derive from other PP than the 3rd and 4th PP, as it happens in bony fish, birds and mammals. In cartilaginous fish, the most primitive thymus-bearing species (for instances sharks), thymus anlagen are located in the 2nd to the 6th PP; in frogs, they are found in the 2 PP and in reptiles, the 2/3 PP (Rodewald, 2008). There are also differences in the number and in the final anatomical position of these organs among vertebrates. Why such anterior to posterior diversity in the number of PP with potential to form a thymus exists within nature has become of great interest for evolutionary developmental biology to study evolutionary conserved molecular mechanisms occurring in early stages of 3/4 PP development.

I.3. The Hox-code in the pharyngeal region

The specification of the body plan was unravelled with the discovery of a clustered family of transcriptional factors, the Homeobox (Hox) genes. They are homologous to the Drosophila homeotic selector genes (Hom-C genes) and highly conserved within phyla. In vertebrates, this complex is usually composed of 39 Hox genes organized into four separated chromosomal cluster, *HoxA* to *HoxD*, and the known mammalian genome has 4 copies of this Hox complex (Capecchi, 1997; De Robertis, 2008a,b; Holland & Takahashi, 2005; Holland, 2013; McGinnis & Krumlauf, 1992; Scott, 1992). The order of Hox genes on their respective chromosomes is remarkably similar to their expression pattern, suggesting these genes to be ruled out by a spatially collinear way of gene expression along the antero-posterior axis of the embryo and determined primarily by the most posterior Hox genes (Duboule & Dollé, 1989; Hunt & Krumlauf, 1992; Krumlauf, 1994; Wilkinson, 1989). Expression pattern of these transcription factors in mouse and chicken suggest the existence of a code whereby particular combinations of Hox genes specify a determined region of the anterior-posterior axis (Duboule & Dollé, 1989; Hunt & Krumlauf, 1991; McGinnis & Krumlauf, 1992; D. J. Roberts et al., 1995). For example, the anterior expression boundary of the paralogous group 2, 3 and 4 *Hox* genes coincide with the 2nd , 3rd and 4th PP regions, respectively (see Figure 4) (Creuzet, Couly, Vincent and L. Douarin, 2002; Hunt & Krumlauf, 1991; Manley & Capecchi, 1995). In figure 4, it is also possible to define two Hox-regions: a negative one throughout the midbrain and ending specifically in the neural tube 1st rhombomere (r) and the 1st PA; and a positive region starting

in the neural tube, specifically in rhombomere 2 and 2nd PA (Creuzet et al., 2002; N R Manley & Capecchi, 1995).

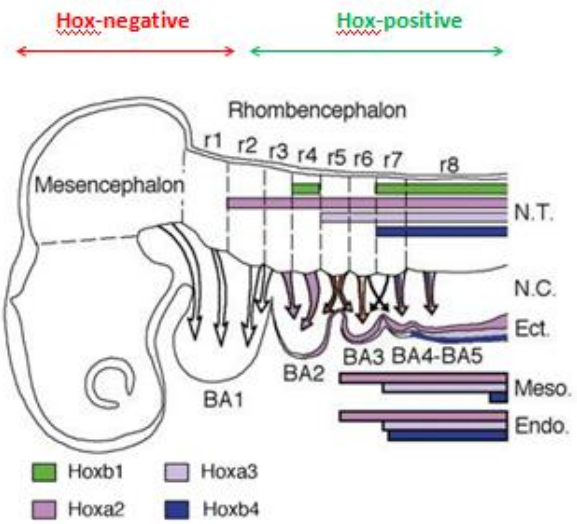

Figure 4 | Schematic representation of Hox genes expression in E3 chick and E2.5 quail embryos. Pharyngeal arches (here described as branchial arches, BA) are being colonized by neural crest cells originated from the posterior half of the mesencephalon and the rhombencephalon, specifically from rhombomeres r1 to r8. Arrows indicate the origin of the neural crest cells migrating to each BA. Expression of Hox genes in the ectoderme, mesoderm and endoderm is also indicated. N.T., neural tube; r, rhomnomere; N.C., neural crest; Ect., ectoderm; Meso., mesoderm; Endo., endoderm. [adapted from Creuzet *et al.*, 2002]

These evidences raised the hypothesis that PP identity, from the 2 PP onward, may be defined by an orderly *Hox* genes expression, and consequently specifying a Hox-code to thymus positional identity. In an evolutionary point of view, the diversity observed in different jawed vertebrate species, on the number of PP with thymus-potential, could be explained by the conservation of this code in the pouch, as a repetitive morphogenic unit.

I.3.1. The hox-code in thymus organogenesis

Many studies in mammal and in birds have unraveled to role of the Hox-code in NCCs and in the PA region. As described above, the expression pattern of the paralogous Hox group 3 is at the level of the 3PP, thymus and parathyroid glands' embryonic origin.

In 1991, Chisaka and Capecchi demonstrated for the first time the phenotypic result of loss-of-function of *HoxA3* in mice (previously identified as Hox-1.5). Similar to DiGeorge's syndrome patients, *HoxA3* mutant mice were athymic, with no paratyroids, with thyroid hypoplasia and multiple defects in the 3rd and 4th PA. Moreover, these mutants presented fusion of the 2nd and 3rd PA and impaired development of 4th PA (Chisaka & Capecchi, 1991). Later, Manley and Capecchi demonstrated that the thyroid defects included hemiagenesis (absence of one of the lobes) and reduction or absence of C cells in the thyroid lobes. C cells are calcitonin-producing cells that are produce in the ultimobranchial bodies. In *HoxA3* mutants, these bodies fail to fuse with the thyroid, explaining the lacking of C cells. The expression pattern of the

paralogous Hox3 group in E10.5 mice embryos was also described: *HoxA3* was strongly expressed in the 3/4 PP endoderm and throughout the mesenchymal cells of the 3 PA; *HoxB3* is primarily expressed in more lateral regions of the 3rd PA mesenchyme; and *HoxD3* is expressed in only a small subset of dorsally located cells in the 3rd PA mesenchyme. Double mutants *HoxA3*$^{-/-}$*HoxB3*$^{-/-}$ and *HoxA3*$^{-/-}$*HoxD3*$^{-/-}$ presented the same exacerbated defects in thyroid and ultimobranchial bodies as the *HoxA3*$^{+/-}$ mutant. Furthermore, *HoxB3*$^{-/-}$*HoxD3*$^{-/-}$ mice did not present obvious defects in the thymus and parathyroid glands. However, in *HoxB3*$^{-/-}$*HoxD3*$^{-/-}$*HoxA3* $^{+/-}$ mutants both organ primordia failed to migrate correctly (N R Manley & Capecchi, 1995, 1998).

In chicken, a similar expression pattern was described for *HoxA3*. It was also demonstrated the similarity between chicken and mouse *HoxA3* control regions and suggested a nested organization of early elements of segmental patterning (Manzanares et al., 2001). It was also demonstrated that depletion of *HoxA3* resulted in defects in the branchial nerve of the 3 PA (Watari-Goshima & Chisaka, 2011).

The complex phenotype presented in mouse and chicken mutants for *HoxA3* demonstrate how important this gene is in multiple processes in the pharyngeal region and how it can regulate interactions between different tissues. Even though some of the defects described are mostly related to alterations in the NCC, absent thymus and parathyroid glands in mutant *HoxA3* could not be explained by NCC defects, since these organs epithelium is endoderm-derived. Moreover, *HoxA3* was recently reviewed as one of the transcription factors controlling early steps of thymus development in mouse, before thymus-specific transcription factor *Foxn1* is expressed (Manley & Condie, 2010). Therefore, we may hypothesize a boundary in the 3/4 PP in which *HoxA3* is establishing the positional identity of the thymic and parathyroid epithelium.

As already mentioned, Hox genes are ruled out by a posterior prevalence, meaning most posterior genes impose their expression, overlapping the anterior Hox gene, resulting in homeotic transformation. Considering our hypothesis that specific hox-code is determining different PP, we would expect duplication of the 2 PP identity in the 3rd, in Hox3 mutants, and duplication of the 3 PP in the 4th, in Hox4 mutants. Unfortunately, the complex phenotype these mutants present would make it impossible to reveal the effect of altering the Hox-code in that specific pouch, as the observable defects resulted from the alteration of multiple interacting-tissues in that region (endoderm, mesoderm, ectoderm, NCC derived mesenchyme) (Creuzet et al., 2002). Nevertheless, paralogous genes expressed in the specific pouch have to be taken in account, as they could have redundant roles.

However, homeotic transformation of other tissues of the arch region in chick embryos has already been described. Le Douarin and collaborators demonstrated that NCC of the 2 PA obey the "Hox-code posterior prevalence rule" as *HoxA2* mutant mice exhibit homeotic transformation of the 1 PA (Hox-negative) in the 2 PA, giving rise to skeletal elements from cephalic NCC. Moreover, they demonstrated that overexpressing *HoxA2* in the 1 PA led to the transformation of this arch in the 2nd one (Couly et al., 2002; Creuzet et al., 2002).

To sustain this hypothesis of a specific Hox-code established in endoderm is also important to consider the emerging importance of positive auto- and cross-regulatory interactions between Hox genes as a general mechanism for maintaining their correct spatial patterns, as previously

reported in the vertebrate nervous system (Manzanares et al., 2001). Also, trans-regulatory interaction between Hox genes, in order to establish pouch identity, should not be overlooked. Treatment with retinoic acid (RA) lead to an anterior shift of HoxB1 (normally restricted to the endoderm and mesoderm caudal to 4PP) to a level just below 1 PA, disrupting normal development of the most anterior pouches (Mark, Ghyselinck, & Chambon, 2004; Roberts, Ivins, Cook, Baldini, & Scambler, 2006)

How these "positional Hox-code" in endoderm relates with other early patterning transcription factors involved with thymus development is still unknown. Nevertheless, these evidences suggest the Hox-code responsible for thymus positional identity in the 3/4 PP should be *HoxA3*$^{+}$*HoxB1*$^{-}$.

II. Objective

The principal objective of this work was to unravel a possible Hox-code responsible for thymus positional identity.

To study the Hox-code, our first aim was to characterize the normal pattern of Hox genes expression in the pharyngeal region of chicken embryos. Specifically, we evaluated by *in situ* hybridization, Hox genes expression pattern in the prospective domain of the thymus, the 3/4PP endoderm of chicken embryos at E3 and E4 - stages prior to thymus formation.

Our second aim was to genetically modify Hox-code in distinct PP, using the *Tet-off* system from the "Tol2-mediated gene transfer" and "Tetracycline-dependent conditional expression" combined system of vectors. Specifically, our goal was to ectopically express HoxA3 (normally expressed in the 3 PP) in the 2 PP endoderm and to express HoxB1 (normally expressed in the 4 PP) in the 3 PP endoderm. With this approach, we intended to perform a "gain-of-potential" (HoxA3 overexpression) and "loss-of-potential" (HoxB1 overexpression) to produce a thymus in the 2nd and 3rd PP, respectively.

To achieve this second aim, we first produced a *HoxA3* expressing vector, the pT2k-HoxA3eGFP, to be integrated in the combined *Tet-off* system of vectors, the"Tol2-mediated gene transfer" and "Tetracycline-dependent conditional expression". Secondly, we evaluated the efficiency of this system of vectors by *in vitro* transfecting two different mammalian cell lines, the human embryonic kidney (HEK) 293T and the murine 3T3 lines. GFP expression was monitored by fluorescence microscopy observation and analysed by flow cytometry.

III. Experimental design for the study of Hox-code in thymus identity

III.1. The "Tol2-mediated gene transfer" and "tetracycline-dependent conditional expression" system of vectors for the study of Hox genes in thymus development

In 2007, Y. Takahashi and collaborators developed a transposon-mediated gene transfer technique, taking advantage of the *Tol2* transposable element, and combined it with a tetracycline-induced conditional expression system (Sato et al., 2007; Watanabe et al., 2007) (Figure 5). This combined system, which will be used in this work, allows the stable integration and conditional expression of a transgene in chicken embryos, in a stage-specific fashion.

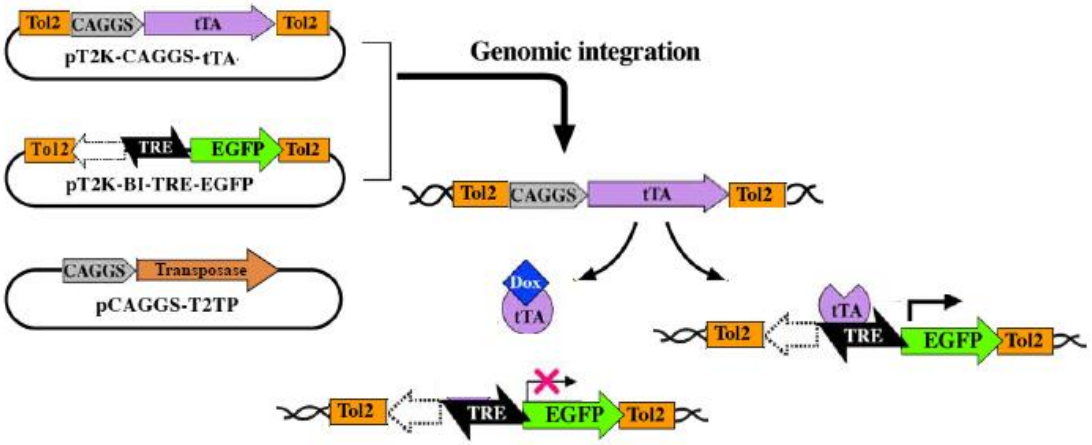

Figure 5 | The "Tol2-mediated gene transfer" and "tetracycline-dependent conditional expression" *Tet-off* combined system. Transient activity of transposase (pCAGGS-T2TP) will induce the transposon construct containing rtTA2S-M2 (pT2K-CAGGS-rtTA2SM2) and TRE-eGFP (pT2K-BI-TREeGFP) to be integrated into the host genome. Activation of transcription of the TRE-driven gene ("tet-on") occurs only in the absence of doxycycline (Dox). [Adapted from Sato *et al.*, 2007]

This system is composed of the following plasmids: 1) pT2K-CAGGS-tTA2, 2) pT2K-BI-TREeGFP and 3) pCAGGS-T2TP. Plasmids 1 and 2 were both constructed with a gene expression cassette delimited by *Tol2* transposable elements. When these three plasmids are electroporated or transfected into a embryo or cell culture, the third plasmid pCAGGS-T2TP, which transiently expresses the transposase, will induce the transposon construct containing either CAGGS-tTA (plasmid 1) or TRE-eGFP (plasmid 2) to be integrated into the host genome. Then, the tet-controlled transcriptional activator (tTA – plasmid 1), under the control of CAGGS promoter, will act on the *cis*-element promoter, the tetracycline responsive element (TRE) of the second plasmid, therefore activating transcription of the TRE-driven gene. tTA can only bind to TRE in the absence of doxycycline (doxy, an analog of tetracycline). When doxy is present in this system, it will bind to tTA, blocking its ability to recognize and bind to TRE. The TRE promoter region of the pT2K-BI-TREeGFP is bidirectional with two minimal promoters of cytomegalovirus in both directions, having an eGFP sequence in one direction and a polylinker region on the

other one, where it is possible to clone the transgene of interest. Thus, cells expressing the transgene can be identified by GFP expression.

To investigate the possible Hox-code give thymus positional identity for it to develop we aim to modify the Hox-code in the 2nd and 3rd PP endoderm. These endoderm pouches will be genetically modified to express *HoxA3* and *HoxB1*, respectively, using the "*Tol2*-mediated gene transfer" and "Tetracycline-dependent conditional expression" combined system of vectors, in a functional assay to thymus formation. Therefore, coding sequences for *HoxA3* and *HoxB1* are intended to be sub-cloned in the pT2K-BI-TREeGFP in order to produce the pT2K-HoxA3eGFP and pT2K-HoxB1eGFP constructs. For this project, the pT2K-HoxA3eGFP construct was already developed (see section III.3.Materials and Methods for details).

III.2. Quail-chick chimeras for the study of Hox-code in the positional identity of the thymus - functional assay to thymus formation

In order to genetically modify the Hox-code in the 2nd and 3rd PP endoderm, we designed a functional assay for evaluation of thymus formation. Isolation of the endoderm of the 2 PP and 3/4 PP would be performed in E2.5 and E3 quail embryos, respectively, as previously described (NM Le Douarin & Jotereau, 1975). These isolated endoderms would then be genetically modified by electroporation with pT2K-HoxA3eGFP and pT2K-HoxB1eGFP, respectively, integrated in the combined system of vectors described above. Afterwards, electroporated quail's 2 PP and 3/4 PP endoderm would be cultured in association with somatopleural mesenchymal tissues isolated from E2.5 chick embryos, generating a chimeric tissue co-culture. After an incubation period, these chimeric co-cultures would be grafted onto a chorioallantoic membrane (CAM) and left for develop.

With this functional assay we expect the formation of a thymus from the genetically altered 2 PP ("gain-of-potential" by overexpression of HoxA3) and the genetically altered 3/4 PP not to produce a thymus ("loss-of-potential" by overexpression of HoxB1).

At the time of this thesis dissertation, the functional assay has not been performed.

III.3. Materials and Methods

III.3.1. Molecular biology procedures

Bacteria preparation and transformation

All bacterial transformations in this study were performed using the DH5-α strain of *E. coli.* Before transformation, and to allow the intake of exogenous DNA, cells have to go through a process to become competent cells. Non-competent *E. coli* DH5-α from frozen glycerol stock were plated onto LB plates, supplemented with ampicilin (100 µg/mL) and grown o/n. One colony was selected for a starter culture. The next day a higher volume of LB was inoculated with 1/100 dilution of the starter culture and incubated until it reached 0.3 optical density at 600 nm (OD_{600}). The cells were kept on ice and harvested by a series of centrifugations in the

presence of $CaCl_2$ to generate chemically competent DH5-α cells. Transformation of DH5-α cells was performed by heat shock treatment for 1 min. Detailed protocols for both preparation and transformation of DH5-α cells are shown in Appendix II.

Isolation of total RNA

Total RNA extraction from chicken embryos with 3 days of development was performed using High Pure RNA Isolation Kit (Roche) according to the manufacturer specifications. Embryos were cut in pieces and resuspended in 200 µL PBS. After adding 400 µL of Lysis/Binding Buffer and mixing 15 sec with a vortex, the samples were maintained at -20°C until performing to the RNA extraction protocol. The RNA pellet was eluted in 50 µL of Elution Buffer). RNA samples were stored at -80°C.

Complementary deoxyribonucleic acid (cDNA) synthesis

The synthesis of the first-strand cDNA from total RNA (previous section) was carried out using the SuperScript® III First-Strand Synthesis System for RT-PCR (Invitrogen), according to the manufacturer instructions. 2 µg of total RNA were used in each reaction. cDNAs were stored at -20°C until needed.

PCR amplification

cDNA template synthesized from cE3 RNA (previous section**)** was amplified by PCR in a 25 µl reaction with 0.5 µM final concentration of primers, using the Phusion™ Master Mix with HF Buffer (Finnzymes), according to instructions from the manufacturer. The cycling conditions for *HoxA3*, *HoxB2* and *HoxB4* were: 1 cycle to initiate denaturation at 98°C for 15 sec; 30 cycles of denaturation at 98°C for 10 sec, annealing at optimal temperature (see below) for 30 sec, and extension at 72°C for 15 sec per 1Kb; and 1cycle of final extension at 72°C for 10 min. The optimal conditions of *HoxA3* amplification was 65°C for annealing temperature and 15 sec for extension (1251 bp production). Optimal conditions for *HoxB2* and *HoxB4* were 58°C of annealing temperature and 15 sec for extension (579 bp production for *HoxB2*; 742 bp production for *HoxB4*). Samples were stored at -20°C. For the PCR reaction MyCycler™ Thermal Cycler (Bio-Rad) was used.

Primers selection for amplification of chicken *HoxA3*, *HoxB2* and *HoxB4* sequences

Chicken *HoxA3* sequence

HoxA3 mRNA sequence in chicken was identified by Watari-Goshima & Chisaka (2011). Partial nucleotide sequence of *HoxA3* in *Gallus gallus* is shown below (the sequences chosen for primers construction are in bold, the coding sequence is underlined and the stop codon that corresponds to the end of the HOXA3 protein is in red):

HoxA3 Gallus gallus gene ID: NM_204548.1:

1681 agtttgcgaa ataaatattg ggaaacaacg aa**atgcaaaa agcgacctac tacg**acagct
1741 ctgcaatcta tggtgcctac ccctaccaag gagcaaatgg tttcacttat aatgcgagtc
(…)
2881 catacacaga ccttacagct caccatcctt ctcagggaag aattcaggaa gcgcccaaa**c**
2941 **tcacccatct gtaggagcca ggag**tcacta ggcggaacgc aaagccccaa ccttttaaag

To amplify the *HoxA3* sequence, and allow direct cloning and its further expression the sequence of the 5' primer was modified introducing a restriction site and a KOZAK sequence. The final primers were: forward 5'-GCTAG**CCATG**caaaaagcgacctactacg-3' (the inserted sequences are in capital letter; the restriction sequence of *NheI* is underlined; the KOZAK sequence is in bold) and reverse 5'-ctcctggctcctacagatgggtgag-3'. The expected amplified product is 1251 bp.

Chicken *HoxB2* sequence

HoxB2 mRNA sequence in chicken was predicted by automated computational analysis. For human and mouse, this sequence was already identified and referenced so we performed a blast analysis between the predicted chicken *HoxB2* sequence and the *HoxB2* mRNA sequences for human and mouse. We found that only the 5´ region was homologous for the 3 species (approximately by 70%), so the reverse primer was designed from the most homologous stretch in 3' termini.

Partial nucleotide sequence of *HoxB2* in *Gallus gallus* is shown below (the sequences chosen for primers construction are in bold and the coding sequence is underlined):

HoxB2 Gallus gallus gene ID: XM_003642792.1:

61 cctccttcct ccccccctccc gctttttaaa ccctgggccc tggaaaagcc **atgaattttg**
121 **aatttgagag** ggagatcggg tttataaata gccagccttc gctcgcagag tgcctgacgt
(...)
601 acctctgcag gccccgtcgg gtggaaatcg cggctttgct cgacctgacc gagcgacaa**g**
661 **tcaaagtgtg gttccagaac cgcaggatga** agcacaagag gcaaacacag tacaaagaac

To amplify the *HoxB2* sequence, and allow direct cloning and its further expression the sequence of the 5' primer was modified introducing a restriction site and a KOZAK sequence. The final primers were: forward 5'-GCTAG**CCATG**aattttgaatttgagagggagatcggg-3' (the inserted sequences are in capital letter; the restriction sequence of *NheI* is underlined; the KOZAK sequence is in bold) and reverse 5'-tcatcctgcggttctggaaccacactttgac-3'. The expected amplified product is 579 bp.

Chicken *HoxB4* sequence

HoxB4 mRNA sequence in chicken was identified by Attia *et al.* (2009). Partial nucleotide sequence of *HoxB4* in *Gallus gallus* is shown below (the sequences chosen for primers construction are in bold, the coding sequence is underlined and the stop codon that corresponds to the end of the HOXB4 protein is in red):

HoxB4 Gallus gallus gene ID: NM_205293.1:

241 atatatatat atatattttt cgtgtgtgca attctaagaa atta**atggcc atgagctcgt**
301 **ttttgatcaa** **ctc**caactat gtggacccca agttcccacc ctgtgaagag tattcccaca
(…)
961 gcctgcagat cccaccggca gcttctcaaa gcc**gatccag cggaccagcc agcagccta**t
1021 **aa****ctatt**ccc tggaggattt cagggcccgt tgtcgtatgg cagtgccgga ggtgggggtg

To amplify the *HoxB4* sequence, and allow direct cloning and its further expression the sequence of the 5' primer was modified introducing a restriction site and a KOZAK sequence. The final primers were: forward 5'-GCTAG**CCATG**gccatgagctcgtttttgatcaactcc -3' (the inserted sequences are in capital letter; the restriction sequence of *NheI* is underlined; the KOZAK sequence is in bold) and reverse 5'-aatagttataggctgctggctggtccgctggatc-3'. The expected amplified product is 742 bp.

DNA Restrictions

Enzymatic restriction of DNA was performed using commercially available restriction enzymes and respective buffers (Promega, New England Biolabs), at 37°C, for 2h to 3h, the volume of reaction depended on the quantity of DNA (as a rule final volume should be 10x higher (in µL) than the quantity of DNA (in µg)). For each reaction the volume of enzyme used never surpassed 10% of the total reaction volume.

TOPO II PCR cloning

PCR products were cloned into TOPO II PCR vector using Zero Blunt® TOPO® PCR Cloning Kit (Invitrogen) according to manufacturer instructions. Afterwards, the mix was used to transform commercial competent DH5α bacteria. It was the added 250 µL of S.O.C. medium (TOPO® PCR Cloning Kit) and transformed cells were incubated in a 37°C shaker for 45 min (200 rpm). Bacteria were plated (20 µL and 200 µL) on solid LB agar medium supplemented with ampicillin (100µg/mL) (Sigma) and 30 µL of X-Gal (50mg/mL) (Promega) and were incubated at 37°C o/n. Plasmid DNA was extracted (see section Plasmid DNA Mini Preparation and Midi Preparation). Restriction analysis was performed to confirm the correct construction and correct PCR amplification product.

Cloning of *HoxA3* into the pT2K-BI-TREeGFP to generate pT2K-HoxA3eGFP

A second cloning reaction was performed to create the final recombinant plasmids. 4 µg of TOPO-HoxA3 and 5 µg of pT2K-BI-TREeGFP were digested with *Eco*RV and *Nhe*I restriction enzymes, in a total volume reaction of 80 µL and 70 µL, respectively. Afterwards, reaction products were loaded on an agarose gel (see section Agarose gel electrophoresis) and DNA fragments of interest were recovered and purified (see section QIAquick gel extraction kit).

The ligation reaction of the linearized vector pT2K-BI-TREeGFP and insert HoxA3 (with the correct termini) was performed according to the ratio: µg of vector/vector's dimension = 10x (µg of insert/insert's dimension). For the ligation reactions it was used 150 ng for both pT2K-BI-TREeGFP (8.7kb) and HoxA3 insert (1,25kb) in a total volume of 20 µL. The reaction was performed in 1x Buffer for T4 DNA Ligase (Biolabs), with 1µL T4 DNA ligase (Biolabs 400U/µL) at room temperature (22°C) o/n. The ligation product was directly used to transform DH5-α competent cells. Plasmid DNA was extracted and isolated (see section Plasmid DNA mini- and midi-preparation) from transformant colonies. The insertion of donor DNA into the vector (pT2K-BI-TREeGFP) was confirmed by double digestion with *Eco*RV and *Nhe*I.

Plasmid DNA mini- and midi-preparation

For mini-preparation of plasmid DNA, single colonies of transformed bacteria were collected and inoculated into 5 mL of liquid LB medium supplemented with ampicillin (100 μg/mL) and incubated in a 37°C shaker (225 rpm) o/n. The purification of plasmid DNA was carried out using the QIAprep® Spin Miniprep Kit (QIAGEN) according to the protocol recommended by the manufacturer.

For midi-preparation of plasmid DNA, single colonies of transformed bacteria were grown o/n in 50 or 100 mL (high or low copy, respectively) of liquid LB medium supplemented with ampicillin (100 μg/mL) at 37°C (225 rpm) o/n. The purification of plasmid DNA was carried out using the QIAfilter Plasmid Midi kit (QIAGEN) according to the protocol recommended by the manufacturer. DNA samples were stored at -20°C.

QIAquick Gel extraction kit

DNA extraction from agarose gel was carried out using the QIAquick Gel Extraction Kit (QIAGEN), according to manufacturer instructions. DNA was eluted with 30μL of DNase and RNase free water.

DNA and RNA quantification

The concentration of nucleic acids was determined by spectrophotometry using the NanoDrop® ND-1000 Spectrophotometer (Thermo Scientific). One A_{260} unit corresponds to 50 μg/ml of double-stranded DNA and to 40 μg/ml of single-stranded RNA. DNA and RNA samples purity was evaluated based on A_{260}/A_{280} and A_{260}/A_{230} ratios. For the A_{260}/A_{280} ratio, ~1.8 is generally accepted as pure DNA and ~2.0 as pure RNA. The A_{260}/A_{230} is a secondary measure for nucleic acid purity. In this ratio, pure DNA and RNA values must higher than the ones in A_{260}/A_{280}, commonly in the range of 1.8-2.2, respectively. Lower ratio values are due to proteins, phenol or co-purified contaminants.

Preparation of riboprobes for *in situ* hybridization

To generate the antisense and sense transcripts, TOPO II PCR, pGEM-T and pGEM-T easy vectors containing the sequences of interest were linearized with the appropriate restriction enzyme (see Table 1 in Appendix II). The digestion reaction was performed in a total volume of 150 μL containing 20 μg of DNA, 15 μL of 10x enzyme buffer, 5 μL of restriction enzyme (6 U-20 U/μL) and RNase-free water. After digestion, linearized plasmid DNA was purified using phenol-chloroform extraction and ethanol precipitation (see Appendix II). The synthesis of digoxigenin (DIG) -labelled antisense and sense RNA probes was carried out by *in vitro* transcription at 37°C for 2h using Riboprobe® Combination System SP6/T7 or T3/T7 (Promega). The reaction contained 8 μL of Transcription Optimized 5x Buffer, 4 μL of 0.1M DTT, 2 μL of each rGTP, rATP, rCTP (10 mM), 1.3 μL of rUTP (10 mM), 2 μL of RNasin® Ribonuclease Inhibitor, 0.7 μL of Digoxigenin-11-UTP (10 mM) (Roche) and 8 μL of RNAse free water. To this mixture solution and 2 μL of the appropriate RNA polymerase (see Table 1 in Appendix II), 2 μL (2μg) of the linearized templates were added. After incubation for riboprobe synthesis, the sample was treated with 6 μL of DNase I recombinant RNase-free (10 U/μL) (Roche) at 37°C for 15 min. Purification of the probe was performed using illustra MicroSpin G-50 Columns (GE

Healthcare) according to manufacturer instructions. To check for probe quality and success of transcription reaction, 2 µL of reaction product were analyzed by agarose gel electrophoresis (see below).The samples were stored at -20°C.

Agarose gel electrophoresis

Electrophoresis in agarose gel was performed to confirm PCR amplification products, complete digestions with restriction enzymes, to recover and purify specific DNA fragments using extraction kit (see section QIAquick Gel extraction kit) and to check riboprobes and DNA samples integrity. UltraPureTM Agarose (Invitrogen) was dissolved by heating in 1x TAE buffer (composition provided in Appendix I*)* to a final concentration of 0.8-1.5% (depending on the required resolution for DNA fragment). To check for the presence of nuclear acids, GelRedTM Nucleic Acid Gel Stain (Biotium) was added to dissolved agarose in a 1:10 proportion. Samples were mixed with 6x Loading Dye or 6x MassRuler™ Loading Dye (both from Fermentas) in 6:1 proportion and were loaded into the gel. Electrophoresis was performed in 1x TAE at 5-10 V/cm of gel length. Samples were observed under UV light and images acquired with AlphaImager HP (Alpha Innotech) or ChemiDoc XRS+ system (Bio-rad). Fragments size was estimated by comparison with the DNA ladders (FastRuler™ Low Range DNA Ladder, FastRuler™ Middle Range DNA Ladder or O'GeneRuler™ 1 kb DNA Ladder, Fermentas) ran along with DNA samples.

III.3.2. Celular biology procedures

Maintenance of HEK 293T and 3T3 cell lines

The Human Embryonic Kidney (HEK) 293T cell line (provided by João Barata's group, *Unidade de Biologia do Cancro*, *Instituto de Medicina Molecular*, Lisbon, Portugal; (Zenatti *et al*., 2011)) and the murine 3T3 cell line (Santos et al., 2007) were maintained in culture medium containing Dulbecco's modified Eagle medium (DMEM) (Gibco) supplemented with 10% FBS (Gibco), 1x Pen/Strep (Gibco), 1x Glutamine (Gibco) and 1x Non Essential Amino Acids (NEAA) (Gibco). The cells were cultured on T25, T75 or T175 flasks (Nunc) using a media volume to surface area ratio of 0.1-0.2 mL/cm^2. All cultures were grown in a humidified incubator (Heraeus® HERAcell®) at 37°C with 5% of CO_2. 293T cells were provided cultured in T25 or T75 flasks. 3T3 cell line aliquotes were taken from the liquid nitrogen and put in a 37°C bath, without immerging, long enough to start to thaw. Immediately after, the cells were resuspended in maintenance medium and plated onto a T75 flask. The medium was changed regularly until cells reached 40-50% confluence. For this, the media was removed and the cells were washed with PBS. In order to detach the cells, pre-warmed 1-2 mL of 0.25% Trypsin/EDTA (Gibco) was added and the cells were incubated at 37°C for about 5 min. When cells detached, trypsin was inactivated by addition of medium. Dilutions were made with the appropriate volume and plated.

Transfection of HEK 293T and 3T3 cell lines

Both HEK 293T and 3T3 cell lines were transfected with a "Tol2-mediated gene transfer" and "Tetracycline-dependent conditional expression" system of vectors, composed by: pCAGGS-

T2TP, pT2k-CAGGS-EGFP, pT2k-BI-TRE-EGFP and pT2k-CAGGS-tTA-M2 (Sato *et al.*, 2007), in 2 different concentrations and in the presence and absence of 2 different concentrations of Doxycycline, in order to study and validate it for our work. A standard calcium phosphate-mediated transfection protocol for mammalian cell lines was used (detailed protocol in Appendix II). For both cell lines, analysis of transfected cells expressing GFP and fluorescence intensity of GFP was performed a different time-points, preliminary by eye observation using a Leica DMIL inverted microscope and quantified by flow cytometry analysis using a BD LSRFortessa cell analyzer. For each condition, $\geq 1x10^4$ cells were analysed with a minimum of 10000 events acquired. Data was analysed with FlowJo (Tree Star, Inc. Ashland, OR). A negative control was employed, where cells went through this transfection protocol but without the addition of plasmid DNA.

III.3.3. Developmental biology procedures

Chicken embryo manipulation

Fertilized chicken (*Gallus gallus*) eggs, obtained from Sociedade Agrícola Quinta da Freiria, S.A., Portugal, were stored at 16°C and incubated at 38°C to initiate development. Embryos age was estimated by incubation time and staged according to Hamburger and Hamilton (Hamburger & Hamilton, 1951). At specific stages of development, embryos were removed and dissected from the egg and the extra-embryonic membranes. Isolated embryos were further processed to whole-mount *in situ* hybridization

Whole-mount *in situ* hybridization

Whole-mount *In situ* hybridization of E3 and E4 chick embryos were performed as previously described (Henrique, 1995 and Etchevers, 2001) (detailed protocol in Appendix II). Whole-mount preparations were hybridized with the follow riboprobes: antisense and sense for HoxA3, HoxB2 and HoxB4; antisense for HoxA2, HoxB1 and HoxB3. Pictures were taken under a Leica Z6 APO equipped with a Leica DFC490 camera.

Whole-mount post-hybridized E3 and E4 chick embryos were fixated and included in paraffin for sectioning throughout embryo's coronal axis. Afterwards, these sections went through Hematoxyline-Eosine (HE) staining. HE staining in paraffin sections was done using Harris Hematoxylin (Merck Millipore) and Eosin Y alcoholic (Thermo scientific) according to manufacturer's instructions. Final preparations were observed and photographed using an Upright Brightfield microscope Leica DM2500, equipped with a color camera for brightfield and differential interference contrast imaging.

IV. Results

IV.1. Patterns of expression of Hox genes in the pharyngeal region of chicken embryos, at stages of development prior to formation of the thymus

To identify the Hox-genes that may be involved in the Hox-code responsible for thymus (and parathyroid glands) positional identity, we first study the expression of hox genes by whole-mount *in situ* hybridization in chicken embryos at E3 and E4.

IV.1.1. Production of new sense and antisense riboprobes

New HoxB2 and HoxB4 riboprobes were produced (sense and antisense). A 579 bp and a 742 bp PCR amplification products of *HoxB2 and HoxB4* were cloned into TOPO II PCR (Figure 6A), respectively (detailed in III.3 Materials and Methods, section Molecular biology procedures).

New HoxA3 riboprobe was produced by cloning a 1251 bp product derived from PCR amplification of *HoxA3* into TOPO II PCR (Figure 6B). This plasmid was further used for the production of pT2K-HoxA3eGFP vector (for functional assay to test "gain-of-potential" of the 2 PP to produce a thymus, detailed in section V.2.1).

IV.1.2. HoxA2, HoxA3, HoxB1, HoxB2, HoxB3 and HoxB4 expression pattern at E3 and E4 chick embryos

HoxA2

In figure 7A, we observed the expression of *HoxA2* in chicken embryos with 3 days of development. *HoxA2* is expressed in the neural tube, at the level of the rhombomeres (r) 2 onwards. As shown in fig.7A' (amplification of the pharyngeal region observed in 7A), *HoxA2* is strongly expressed in the ectoderm and/or mesenchyme of the 2 PA. A more faint expression is observed from the 3 PA onwards. Notice the absence of *HoxA2* expression in the otic vesicle (ov), dorsally positioned to 2 PA. Similar patterns of expression are observed for *HoxA2* at E4 (Fig. 7I and 7I'). These results are in agreement with the expression pattern previously reported (Prince & Lumsden, 1994).

In Fig. 7B and 7J, is depicted the coronal sections of E3 and E4 whole-mount hybridization. In the 2 PA, is confirmed the *HoxA2* expression in mesenchymal cells. Interestingly, the endoderm of the 2 PP showed no *HoxA2* expression in anterior half of the pouch while the posterior half is positive (see green arrows in Fig. 7B). At the level of 3/4 PA, endoderm of the 3/4 PP and mesenchymal cells are faintly positive for HoxA2.

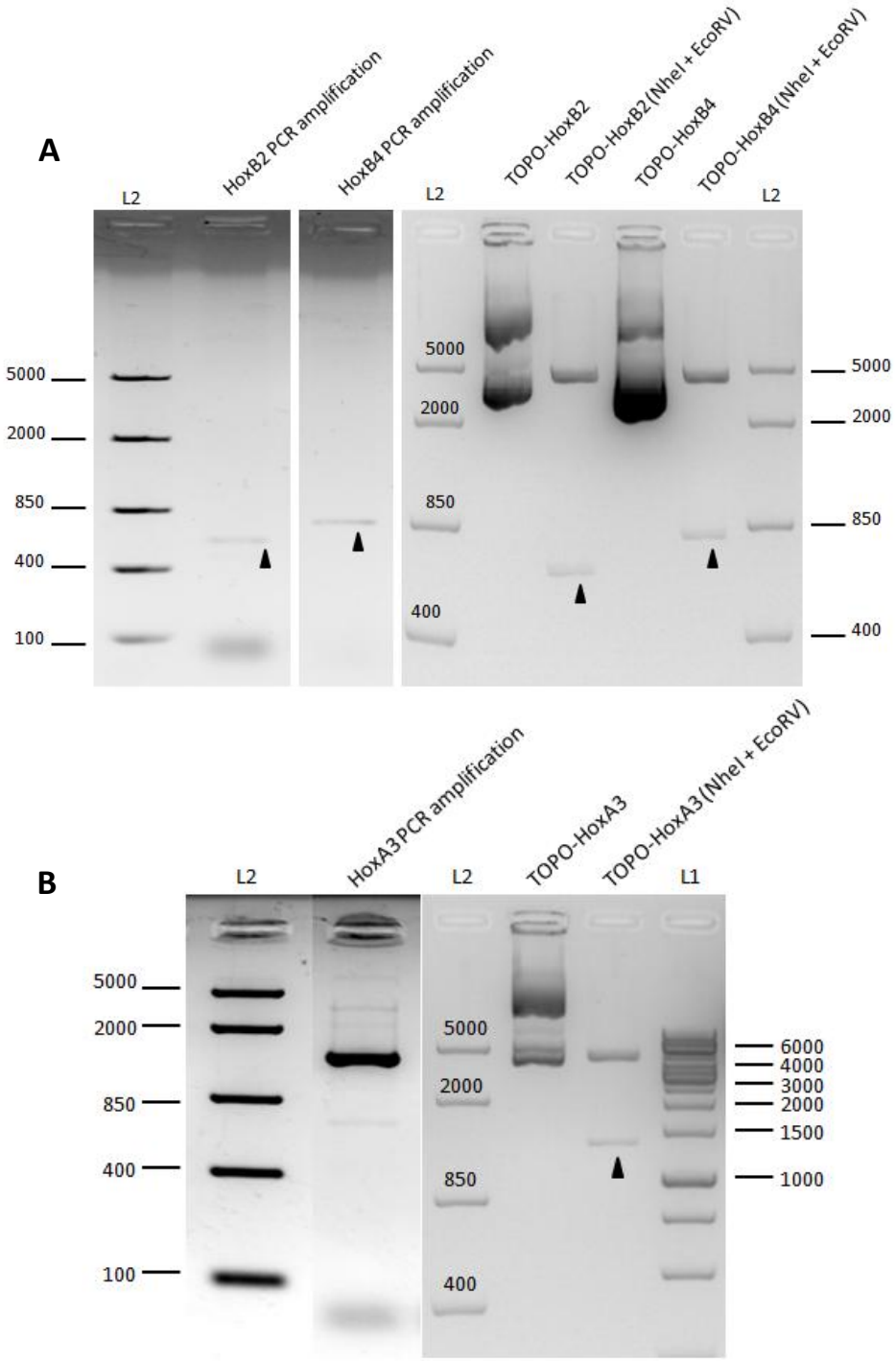

Figure 6 | Agarose gels showing the several steps involved on the generation of TOPO constructs for development of riboprobes. 1.5% (wt/vol) agarose gels showing the steps involved in the construction of TOPO-HoxB2, TOPO-HoxB4 (A) and TOPO-HoxA3 (B). (A) PCR amplification of HoxB2 generated a 579 bp product and PCR amplification of HoxB4 generated a 742 bp product; Cloning of these products in the TOPO vector was confirmed by DNA restriction with NheI and EcoRV of both TOPO-HoxB2 and TOPO-HoxB4, showing a 4000 bp band corresponding to the vector and the band corresponding to the insert. (B) PCR amplification of HoxA3 generated a 1251 bp product. Cloning of this product in the TOPO vector was confirmed by DNA restriction with NheI and EcoRV, showing a 4000 bp band corresponding to the vector and the band corresponding to the 1251 bp insert. Fragment sizes were determined by comparison with O'GeneRuler™ 1 kb DNA Ladder (L1) and FastRuler™ Middle Range DNA Ladder (L2). DNA molecular weight markers are indicated (bp). Black arrows indicate the insert correspondent bands.

HoxA3

Expression pattern of *HoxA3* at E3 is shown in Fig. 7C and 7E (new probe, (t)HoxA3). *HoxA3* is expressed in the neural tube, at r3 level onwards. HoxA3 is strongly expressed in the ectoderm and/or mesenchyme of the 3/4 PA and in the region posterior to 4 PA, as observed in fig. 7C´. Posterior to this region, *HoxA3* is faintly expressed. At E4, *HoxA3* expression pattern is more anteriorly positioned in the pharyngeal region and seems to be highly expressed in the 2/3 PP boundary. *HoxA3* is also expressed in the 3/4 PA (Fig. 7K and 7K'). These results are in agreement with the expression pattern previously reported (Watari-Goshima & Chisaka, 2011).

The coronal sections of E3 and E4 whole-mount hybridization for *HoxA3* are depicted in Fig. 7D and 7L, and 7F and 7N for the new probe. At E3, *HoxA3* expression is confirmed in the mesenchyme cells of the 3PA and, interestingly, in both halves the endoderm of the 3 PP (see orange arrows in fig. 7D and 7F). With the new probe, we also observed and unexpected faint expression of *HoxA3* in the posterior half of the 2 PP (fig. 7F, green arrow). In the most posterior region of the arches, *HoxA3* is also weakly expressed in the mesenchyme of the 4 PA and endoderm of the 4 PP (fig. 7D,L,F,N). In figure 7F (new probe), gene expression is restricted to the most external region of the embryo indicating a permeabilization problem (insufficient proteinase K treatment). At E4, *HoxA3* expression is maintained in the mesenchymal cells of the 3 PA but appears to be absent or faintly expressed in the 3 PP endoderm. The same pattern is observable in the 4 PA and PP.

In figure 9 A is depicted the *in situ* hybridization of the sense riboprobe developed from the new *HoxA3* probe ((t)HoxA3).

HoxB1

HoxB1 expression pattern in chick embryos at E3 and E4 is described for the first time in this dissertation (Figures 7G and 7O). As observed in fig. 7G, *HoxB1* is strongly expressed at r4, is absent in r5, and faintly expressed from r6 onwards. This pattern in the neural tube was previously reported in earlier stages of development (Bothe et al., 2011). In the pharyngeal region, *HoxB1* is only expressed at the level of the 4 PA and onward (Fig. 7G' and O'). In figures 7H and 7P, coronal sections of E3 and E4 whole-mount hybridization are depicted. *HoxB1*, in both stages, is strongly expressed and limited to the most posterior half of the endoderm of the 4 PP (see blue arrows).

HoxB2

Expression pattern of *HoxB2* in chick embryos at E3 and E4 is also described for the first time in this project (Figures 8A and 8G). At the neural tube, *HoxB2* is expressed in r2 onwards which is in agreement with previously reported in earlier stages of development (Barak et al., 2012). In the pharyngeal region, both stages have *HoxB2* expressed in the posterior region to the 4 PA (Fig. 8A' and G'). Coronal sections depicted in figure 8B and 8H confirm that at E3 and E4, *HoxB2* is expressed in the mesenchyme posterior to the 4 PP. *HoxB2* also appears to be weakly expressed in the endoderm of the 4 PP at E4 (fig. 8H, blue arrow).

In figure 9 B is depicted the *in situ* hybridization of the sense riboprobe developed from the new *HoxB2* probe.

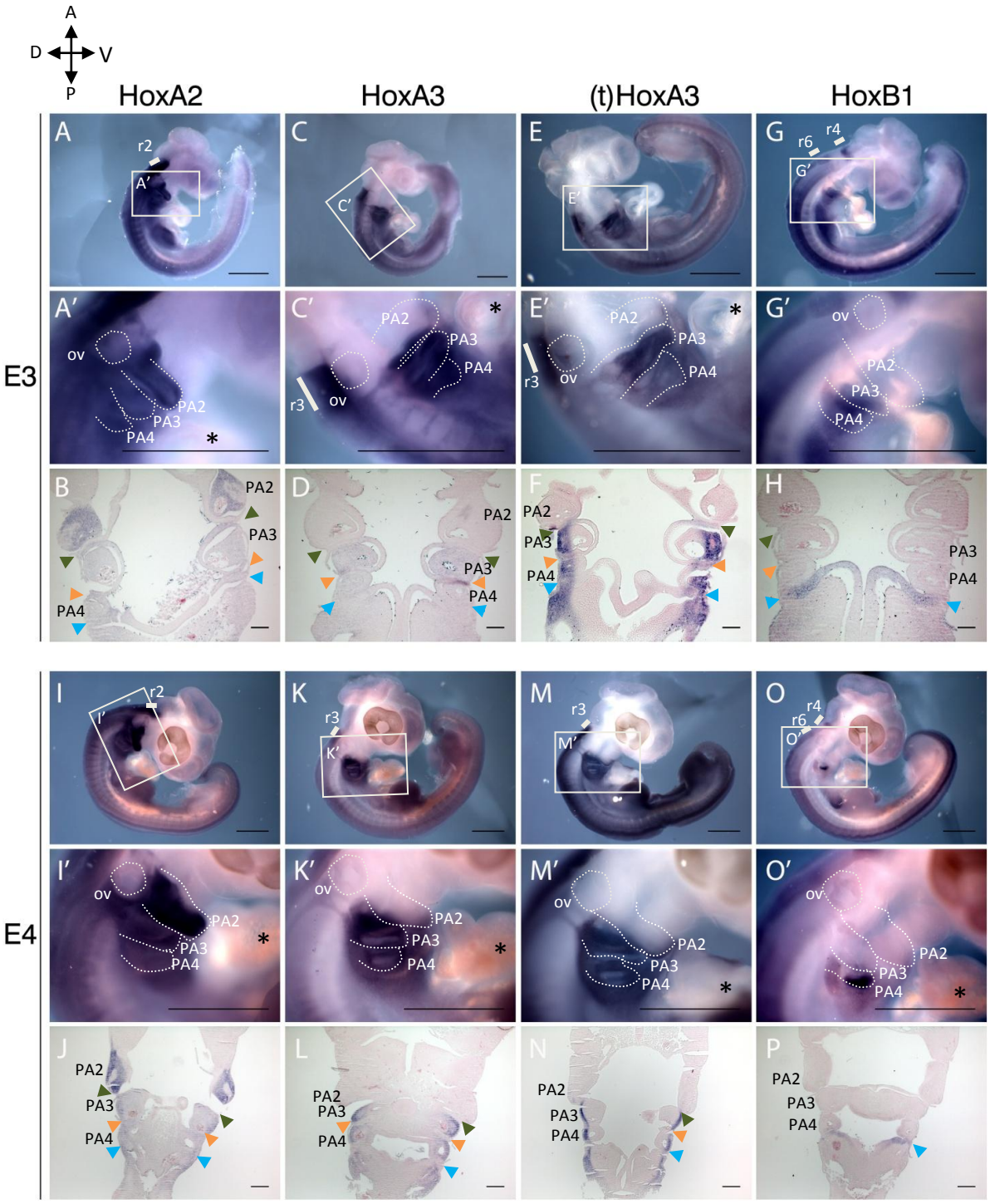

Figure 7 | Expression pattern of *HoxA2*, *HoxA3* and *HoxB1* at E3 and E4 chick embryos. Whole-mount *in situ* hybridization and corresponding post-hybridized coronal section showing the expression pattern of *HoxA2*, *HoxA3* and *HoxB1*. New probe for *HoxA3* is identified as (t)HoxA3. Coronal post-hybridization sections have 5-7 µm and went through HE staining. Different colored arrows indicate a specific PP: green for 2 PP, orange for 3 PP and blue for 4 PP; asterisks indicate the ventral aorta. Scale bars 500 µm (rows A-G' and I-O') and 100 µm (rows B-H and J-P). (A, anterior; D, dorsal; ov, otic vesicle; P, posterior; PP, pharyngeal pouch; PA, pharyngeal arch; r, rhombomere; V, ventral)

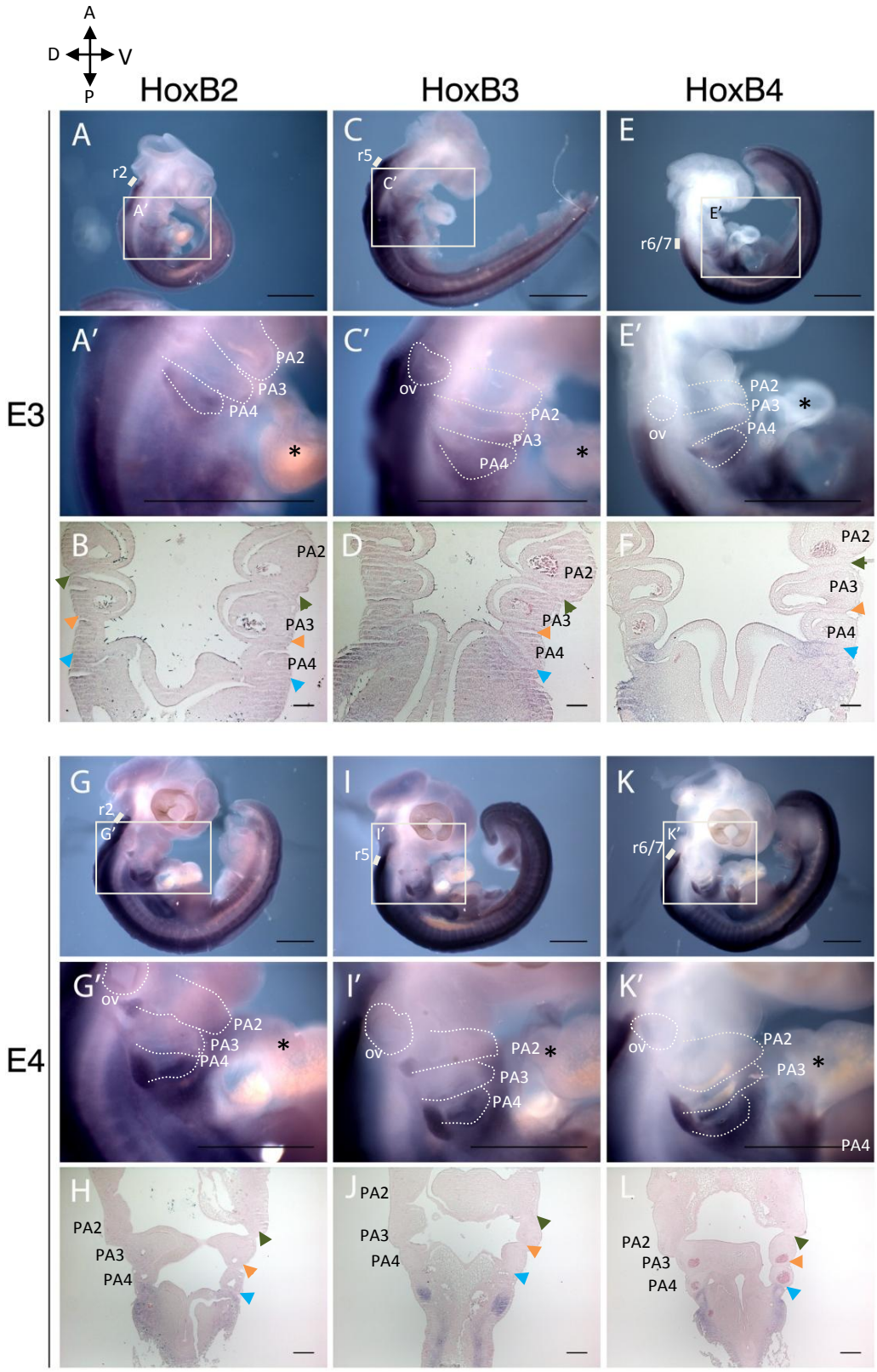

Figure 8 | Expression pattern of *HoxB2*, *HoxB3* and *HoxB4* at E3 and E4 chick embryos. Whole-mount *in situ* hybridization and corresponding post-hybridized coronal section showing the expression pattern of *HoxB2*, *HoxB3* and *HoxB4*. Coronal post-hybridization sections have 5-7 µm and went through HE staining. Different colored arrows indicate a specific PP: green for 2 PP, orange for 3 PP and blue for 4 PP; asterisks indicate de ventral aorta. Scale bars 500 µm (rows A-E' and G-K') and 100 µm (rows B-F and H-L). (ov, otic vesicle; PP, pharyngeal pouch, PP, pharyngeal arch, r, rhombomere)

HoxB3

In figures 8C and 8I is presented the expression pattern of *HoxB3* at E3 and E4. This pattern is described for these stages for the first time in this work. Expression of *HoxB3* in the neural tube is located at r5 onwards and it is in agreement with previously reported in earlier stages of development (Manzanares et al., 2001). Focusing in the pharyngeal region, at E3 and E4 (fig. 8C' and 8I') its expression domain is located posterior to the 4 PA. Curiously at E4 (figure 8I'), *HoxB3* is weakly expressed in the 4 PA.

At E3, *HoxB3* is expressed in the mesenchymal region posterior to the 4 PP, as observed in coronal sections of hybridized E3 and E4 embryos (fig. 8C and 8J). At E4, is strongly expressed in that posterior region and it appears to be faintly expressed in the endoderm of the 4 PP (Fig. 8J, blue arrow).

HoxB4

HoxB4 expression pattern in E3 and E4 is depicted in figures 8E and 8K. Gene expression in the neural tube is at the r6/r7 boundary. This result is in agreement with previously reported in early stages of development (Bel-Vialar et al., 2002). At the pharyngeal region, *HoxB4* is expressed in the 4 PA and in the adjacent posterior region of this arch (figures 8E' and 8K').

HoxB4 expression pattern in coronal sections of E3 and E4 (figures 8F and 8L) confirms expression in the posterior half of the 4 PP and in the mesenchymal region posterior to that pouch.

In figure 9 C is depicted the *in situ* hybridization of the sense riboprobe developed from the new HoxB4 probe.

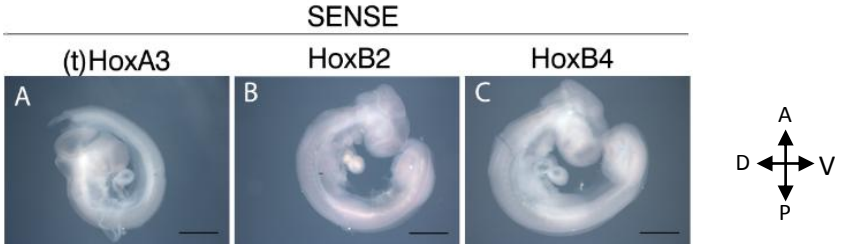

Figure 9 | Whole-mount *in situ* hybridization of E3 chicken embryos with *HoxA3*, *HoxB2*, *HoxB4* sense riboprobes, synthesized from the new TOPO-HoxA3, TOPO-HoxB2 and TOPO-HoxB4 vectors. No detectable signals are observed in E3 embryos hybridized with sense riboprobes for *HoxA3* (new probe, A), *HoxB2* (B) and *HoxB4* (C). Scale bars, 500 µm.

IV.2. In vitro demonstration and validation of the "Tol2-mediated gene transfer" and "Tetracycline-dependent conditional expression" combined system of vectors

To test the efficiency of the combined system of vectors "Tol2-mediated gene transfer" and "Tetracycline-dependent conditional expression", we transfected two mammalian cell lines,

the human embryonic kidney (HEK) 293T and the murine 3T3 lines. These two cell lines were selected for this study due to their high efficiency results when used in multiple transfection protocols.

To assess the best plasmid concentration for the standard calcium phosphate-mediated transfection protocol, two concentrations were tested. In the lowest concentration condition, both HEK 293T and 3T3 cells were transfected with 1.5 µg of pCAGGS-T2TP, 1.5 µg of pT2k-CAGGS-tTA-M2 and 3 µg of pT2k-BI-TRE-EGFP. In the highest concentration condition, both cell lines were transfected with 5 µg ofpCAGGS-T2TP, 5 µg of pT2k-CAGGS-tTA-M2 and 10 µg of pT2k-BI-TRE-EGFP. For both conditions, both transfected cell lines were observed at 24h, 48h and 72h after transfection. Flow cytometry analysis was performed at 72h post-transfection.

The murine 3T3 cell line was analysed by flow cytometry at 72h post-transfection and less than 5% of the cells were GFP positive cells. As a consequence of this low transfection efficiency, no further studies were performed with this cell line.

As observed in Figure 10, at 48h and 72h post-transfection of the HEK 293T cells, there are no significant differences in the number of GFP positive cells and mean fluorescence intensity of GFP for both conditions. By flow cytometry analysis we observed 41.7% and 45% of GFP positive cells in the lowest and highest plasmid -concentration conditions at 72h, respectively. For the following experiments only the lowest plasmid concentration was used.

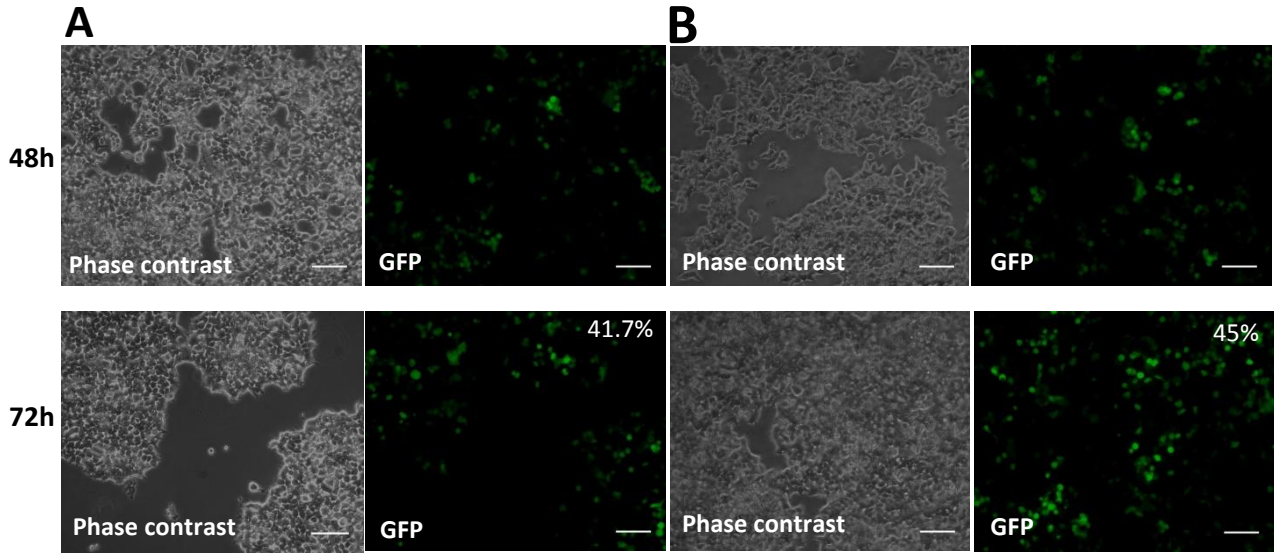

Figure 10 | HEK 293T cell line transfection assay of for best plasmid concentration of the "Tol2-mediated gene transfer" and "tetracycline-dependent conditional expression" combined system of vectors. Cells transfected with 1.5 µg of pCAGGS-T2TP, 1.5 µg of pT2k-CAGGS-tTA-M2 and 3 µg of pT2k-BI-TRE-EGFP (A) and with 5 µg ofpCAGGS-T2TP, 5 µg of pT2k-CAGGS-tTA-M2 and 10 µg of pT2k-BI-TRE-EGFP (B). Microscopic observation at 48h and 72h post-transfection of both (A) and (B) shows no significantly differences between the two plasmid concentrations. Flow cytometry analysis at 72h demonstrated 41.7% of cells expressing GFP in (A) and 45% of cells expressing GFP in (B). Scale bars, 100 µm.

Afterwards, we evaluated the capacity for genomic integration of these vectors (Bi, tA) in HEK 293T cells. Transfected cells were evaluated microscopically and analysed by flow cytometry analysis during the 14 days of culture.

In figure 11 A and B, a significant decrease in the number of cells expressing GFP (more >90%) and in the mean fluorescence intensity is observed throughout the time of culture. From the second to the fifth day after transfection, it was detected a 30% decrease of GFP expressing cells (31.5% to 22.1%). At day 14, only 1.12% of cells were positive GFP. These results show that genomic integration occurs only in a small % of cells and that GFP expression in the first days of culture is majorly transient.

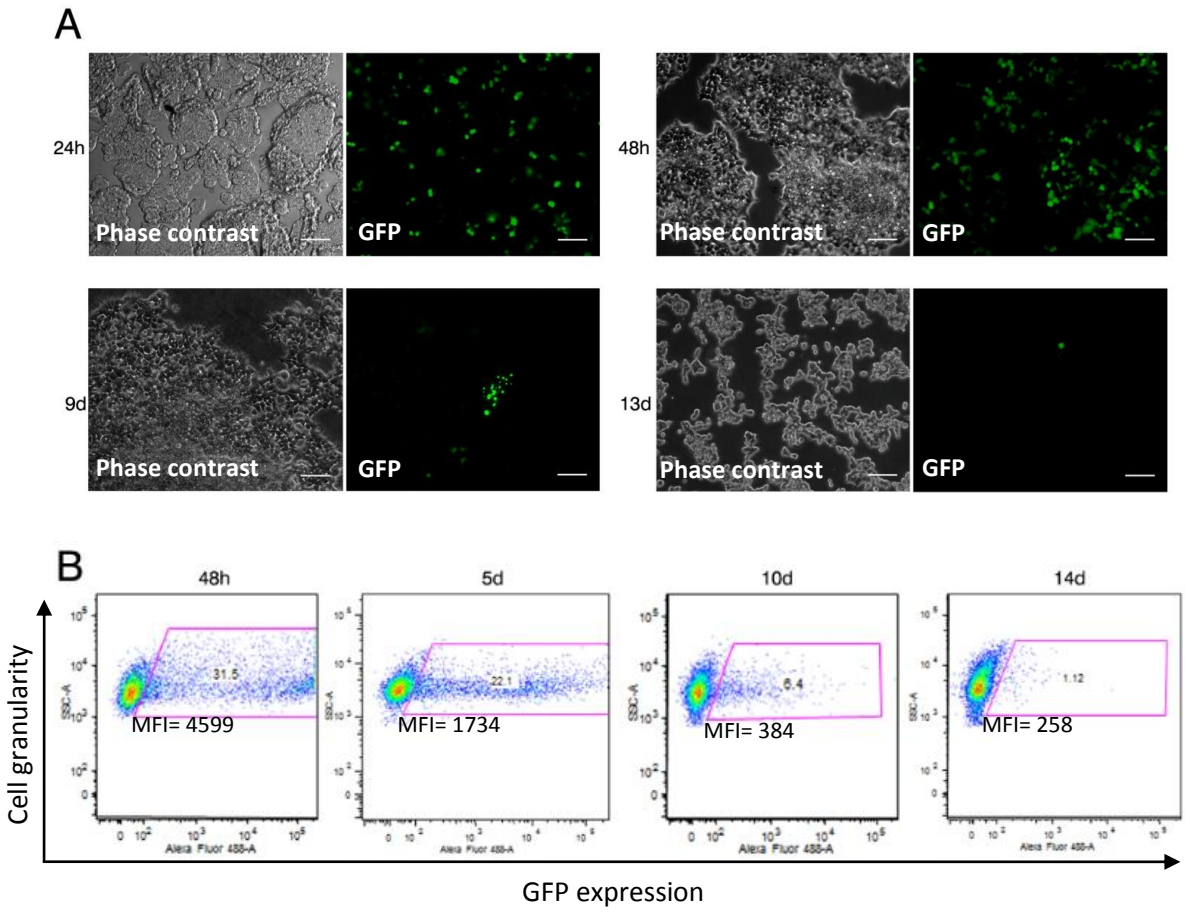

Figure 11 | Evaluation of genomic integration using the "Tol2-mediated gene transfer" and "tetracycline-dependent conditional expression" combined system of vectors. Microscopic observation (A) and flow cytometry analysis (B) of transfected HEK 293T cells were performed throughout a 14 days long-term culture in the time points depicted in this figure. It was observed a continuous decrease of the number of cells expressing GFP and in the mean fluorescence intensity (MFI) of GFP throughout the 14 days, demonstrating that genomic integration only occurs in a small % of cells. Scale bars, 100 µm.

To modulate the combined systems of vectors ("Tol2-mediated gene transfer" and "tetracycline-dependent conditional expression"), we next performed transfections of HEK 293T cells in the presence/absence of doxy. With this system of vectors, the addition of doxy (which binds to tTA) blocks GFP expression.

Two concentration of doxy were used: 1 µg/mL (condition 1) and 5 µg/mL (condition 2). In both conditions, doxy was added to the culture medium immediately after HEK 293T transfection (details in Materials and Methods, section III.3.2) and cells were maintained for 14 days in culture. In Condition 1, doxy was removed from the culture medium at 48h. With this approach, we have evaluated the capacity of the cells to start expressing GFP after doxy removal. In condition 2, doxy was maintained throughout the 14 days of culture with doxy reinforcement every 48h. With this experiment we evaluate the block of GFP expression by continuous doxy administration. Microscopic observation and flow cytometry analysis of transfected cells was performed between 48h and 14d of culture (detailed time-point analysis in Figure 12).

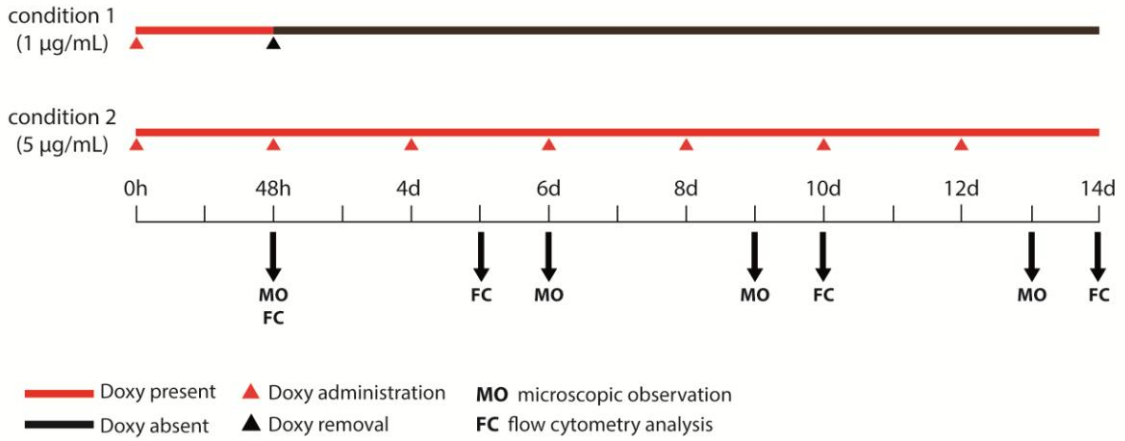

Figure 12 | Experimental design for modulation of the "Tol2-mediated gene transfer" and "tetracycline-dependent conditional expression" combined system of vectors with doxycycline. HEK 293T cells were transfected and maintained in a 14 days culture in the presence of 1 µg/mL (condition 1) or 5 µg/mL (condition 2) of doxycycline (doxy). Transfected cells in condition 1 were maintained in the presence of doxy only for 48h to study the capacity of this system to initiate GFP expression after removal of doxy (black arrow). Transfected cells in condition 2 were maintained in the presence of doxy along the 14d culture to study the blocking of GFP expression, by continuous doxy administration (red arrows). Evaluation of transfected cells in both conditions were performed by microscopic observation (MO) and flow cytometry analysis (FC) at the time-points depicted.

As observed by microscopy (Figure 13), at 48h post-transfection both conditions presented some GFP-positive cells with low fluorescence intensity. However, after doxy removal some bright GFP positive cells were observed at 6, 9 and 13 days of culture in condition 1. Conversely, when doxy was maintained throughout culture (condition 2) no GFP positive cells were observed for the same time-points of culture.

Flow cytometry analysis (figure 14) showed that, approximately, 20% of cells were positive for GFP at 48h-culture irrespectively of doxy concentration used. However, a significant decreased in MFI was observed for both conditions (figure 14 B, MFI~500) when compared with cultures without doxy (figure 11, MFI=4600). At 5 days of culture we observed a reduction in the % GFP positive cells in both conditions, having the condition 2 half of GFP^+ cells when compared with condition 1 (12%). Importantly, the MFI-GFP has increased significantly (doubled) in condition

1 (with doxy removal) while it has decreased significantly (approximately 70%) in condition 2, when compared to 48h-cultures (Figure 11 B). At 10 and 14 days of culture a strong reduction of GFP cells were observed for both conditions (>4%), consistent with previous results of transient expression of GFP in this culture system.

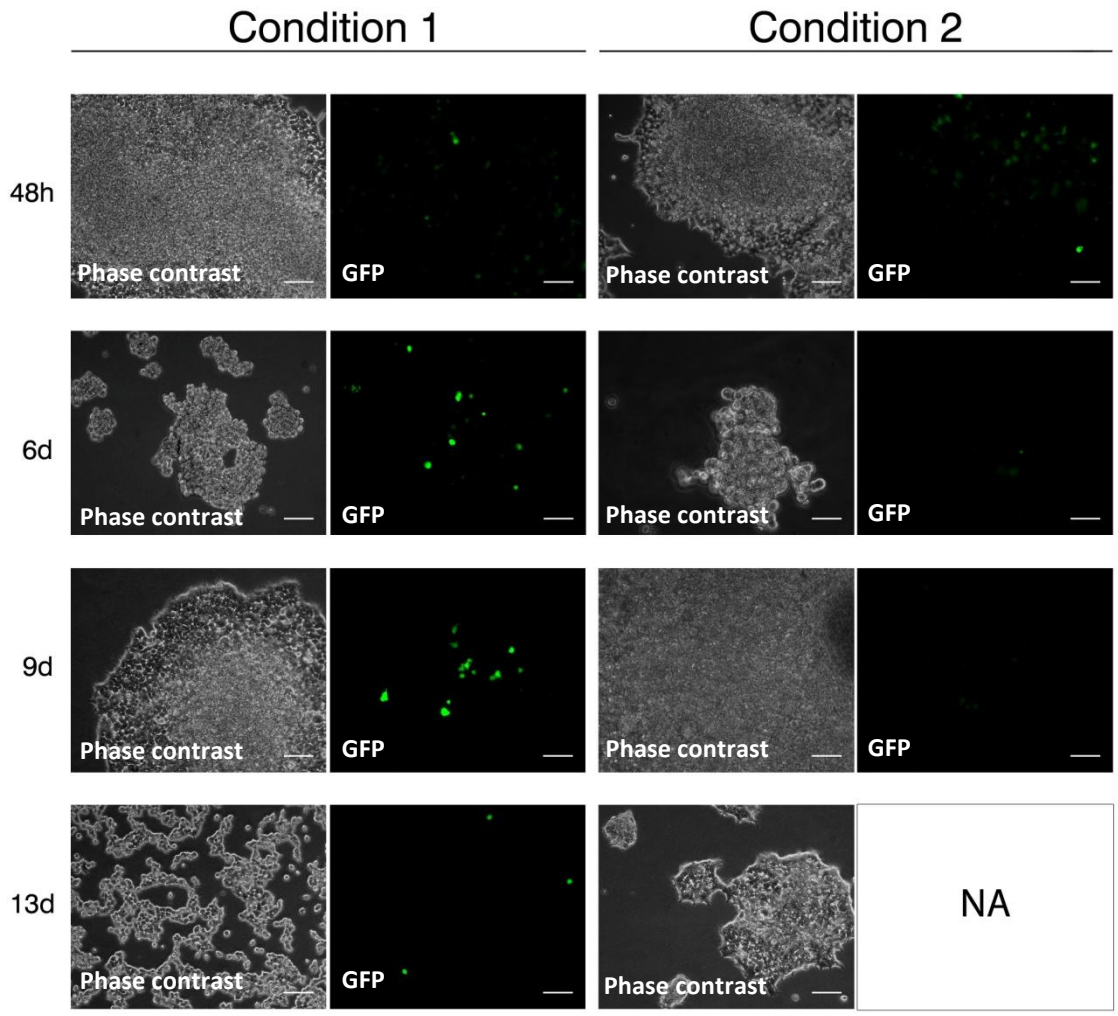

Figure 13 | Modulation of the "Tol2-mediated gene transfer" and "tetracycline-dependent conditional expression" combined system of vectors with Doxycycline – fluorescence microscopy analysis. HEK 293T cells were transfected in the presence of 1 µg/mL (condition 1) and 5 µg/mL (condition 2) of Doxycycline and regularly monitored by microscopic observation (detailed in figure 12). After doxy removal at 48h in condition 1, fluorescence intensity of GFP increased, conversely to transfected cells in condition 2 (maintained in a doxy-culture). NA, not acquired. Scale bars, 100 µm.

A

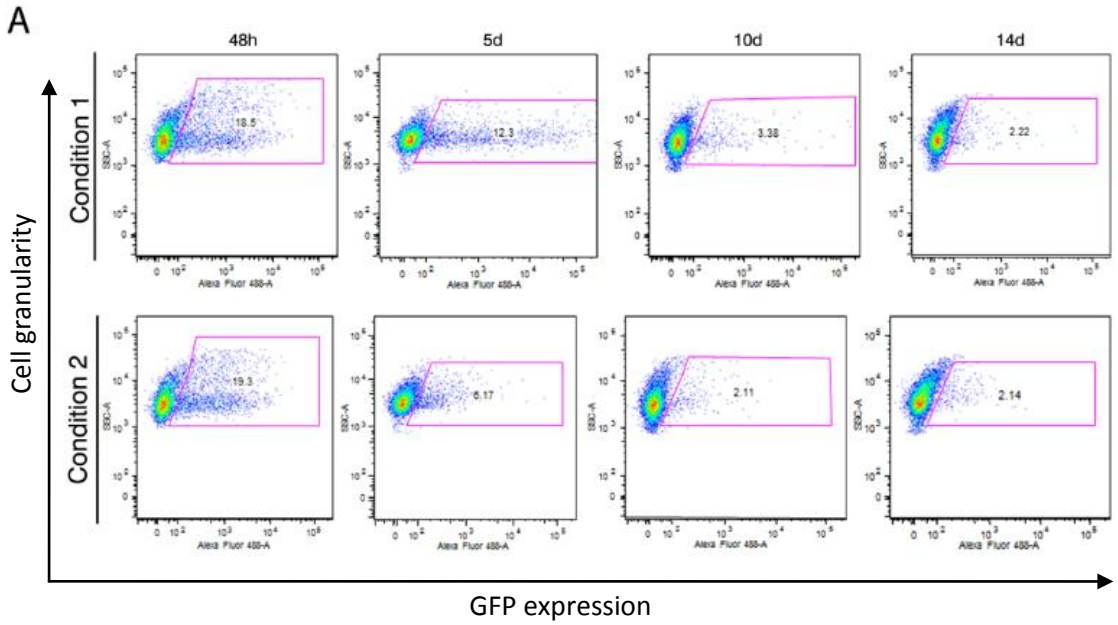

B

	48h		5d		10d		13d	
	%	MFI	%	MFI	%	MFI	%	MFI
Condition 1	18.5	512	12.3	907	3.38	317	2.22	233
Condition 2	19.3	487	6.17	250	2.11	235	2.14	241

Figure 14 | Modulation of the "Tol2-mediated gene transfer" and "tetracycline-dependent conditional expression" combined system of vectors with Doxycycline – flow cytometry analysis. HEK 293T cells were transfected in the presence of 1 µg/mL (condition 1) and 5 µg/mL (condition 2) of Doxycycline and regularly analysed by flow cytometry analysis (detailed in figure 12). (A) Flow cytometry analysis was performed throughout the 14 days long-term culture in the time points depicted. (B) Summary table of flow cytometry analysis. Red line represents the presence of doxy in the system. After removal of doxy at 48h from condition 1, it was detected an increase in the mean fluorescence intensity (MFI) of GFP. In 2, with continued doxy administration, MFI continued to decrease.

Together, these results suggest a 'GFP expression-leakage' in the "Tol2-mediated gene transfer" and "tetracycline-dependent conditional expression" combined system of vectors, when modulated by doxy.

IV.3. In vivo modulation of the Hox-code in the 2nd and 3rd PP endoderm

Whole-mount *in situ* hybridization of E3 and E4 chicken embryos allowed us to define Hox genes expression pattern in the pharyngeal region. The second aim for this work was to genetically modify Hox-code in the 2 PP and 3 PP endoderm. As we can see in figure 7C and 7D, *HoxA3* is expressed in the chick 3 PP endoderm. Therefore, we aimed to perform a "gain-of-potential" of the 2 PP by ectopically express *HoxA3* in the 2 PP endoderm, and test for thymus formation. This gain-of-function of *HoxA3* will be performed using a *Tet-off* system

from “Tol2-mediated gene transfer” and “Tetracycline-dependent conditional expression” combined system of vectors. In this work, we generated a recombinant plasmid by inserting the HoxA3 sequence into the pT2K-BI-TREeGFP vector. Our cloning strategy had three main steps: PCR reaction to amplify the sequence of interest; cloning of the amplified sequence into TOPO II PCR vector and then subcloning it into a pT2K-BI-TREeGFP vector.

IV.3.1. Production of the pT2K-HoxA3eGFP

To produce the pT2K-HoxA3eGFP vector, a 1251 bp product derived from PCR amplification of *HoxA3* was cloned into TOPO II PCR. The digestion of TOPO-HoxA3 with EcoRV and NheI showed two DNA bands: one of 4kb, representing the TOPO II PCR, and the other with 1251 bp, the *HoxA3* insert, confirming the expected cloning reaction. Secondly, we subcloned the EcoRV/NheI *HoxA3* purified insert, from TOPO-HoxA3, in the pT2K-BI-TREeGFP (8.7 kb) digested with *Eco*RV/*Nhe*I. To confirm the integrity of the pT2K-HoxA3eGFP vector, digestion with EcoRV and NheI showed two DNA bands: one of 8.7 kb (the vector) and other with 1251 bp (the insert).

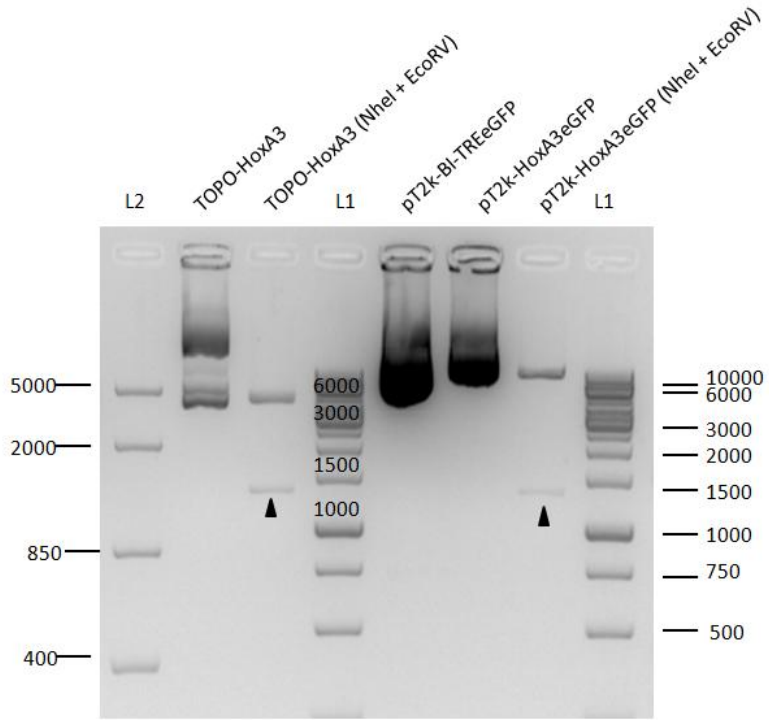

Figure 15 | Agarose gel showing the several steps involved on the generation of the pT2k-HoxA2eGFP. 1.5% (wt/vol) agarose gels showing the cloning steps performed to produce the pT2k-HoxA2eGFP. Cloning of the *HoxA3* PCR product in the TOPO vector was confirmed by DNA restriction with NheI and EcoRV, showing a 4000 bp band corresponding to the vector and the band corresponding to the 1251 bp insert. Sub-cloning of *HoxA3* insert into the pT2k-BI-TREeGFP was confirmed by the same DNA restrictions (NheI and EcoRV) of the pT2k-HoxA2eGFP. Two bands were obtained, one with approximately 9 kb corresponding to host vector (pT2k-BI-TREeGFP) and another with 1,2 kb corresponding to the *HoxA3* insert .Fragment sizes were determined by comparison with O'GeneRuler™ 1 kb DNA Ladder (L1) and FastRuler™ Middle Range DNA Ladder (L2). DNA molecular weight markers are indicated (bp). Black arrows indicate the insert correspondent bands.

V. Discussion

The main objective of this work was to unravel a possible Hox-code responsible for the positional identity of the thymus. To do so, we characterized the expression pattern of several Hox genes along the pharyngeal arches and pouches, at stages prior to thymus development and designed a functional assay of "gain-of-potential" and "loss-of-potential" of the 2 PP and 3 PP, to test formation of a thymus, by ectopically express HoxA3 and HoxB1, respectively.

For the characterization of the expression pattern of Hox genes in the pharyngeal region, sense and antisense riboprobes for *HoxA2*, *HoxA3*, *HoxB1*, *HoxB2*, *HoxB3* and *HoxB4* were synthesized. Whole-mount *in situ* hybridization for these probes and post-hybridization sectioning through the coronal axis were performed in E3 and E4 chick embryos. For this particular study, new sense and antisense probes for *HoxA3*, *HoxB2* and *HoxB4* were developed. Gene expression pattern of the new developed probes were in agreement with previous reports, validating the characterization of these genes expression pattern.

Our functional assay of gain- and loss-of-potential was designed to evaluate thymus formation when over-expressing *HoxA3* in the endoderm of the 2 PP and *HoxB1* in the endoderm of the 3 PP. To do so, our aim was to develop the pT2k-HoxA3eGFP and the pT2k-HoxB1eGFP constructs to combine with the "Tol2-mediated gene transfer" and "Tetracycline-dependent conditional expression" system of vectors. Moreover, we studied the efficiency of this system by evaluating the capacity of genomic integration of these vectors and monitored its response when modulated by doxycycline. Analysis of these parameters was performed by microscopic observation and flow cytometry analysis.

V.1. HoxA3 and HoxB1 as possible Hox-code for thymic rudiment positional identity

The presumptive territory of the thymus and parathyroid glands in endoderm of the 3/4PP has been shown to be limited by *Foxn1* in the dorsal domain and *Gcm2* in the median/anterior domain, respectively, in E4.5 chicken embryos (Neves et al., 2012). In our study, we characterized by whole-mount *in situ* hybridizations the expression of *HoxA2*, *HoxA3*, *HoxB1*, *HoxB2*, *HoxB3* and *HoxB4* in the pharyngeal region of chick embryos at stages prior to thymus formation (E3 and E4) (Figures 7 and 8).

We observed the expression of *HoxA2* in the 2 PA and *HoxA3* in the 3 PA, as previously reported in mice (Manley & Capecchi, 1995; Santagati et al., 2005) suggesting a conservative role of these genes in the pharyngeal region. Specifically, we observed *HoxA3* expression along both anterior and posterior portions of the 3 PP and in the anterior portion of the 4 PP (figure 7D, F, L and N). The role of *HoxA3* in the derivatives of the 3 PA and PP has been long studied in mice. Mutant mice for this gene present several defects in the 3rd and 4th PA and, most interestingly, these animals are athymic. In later studies, *HoxA3* was considered one of the first transcription factors controlling thymus and parathyroid glands patterning in mice, and an upstream regulator of a gene network cascade for initial fate specification (Manley & Condie, 2010).

For the stages of development we have studied, the expression pattern of HoxB genes is not in agreement with this general idea of A-P expression patterning. *HoxB1* is expressed in the 4 PA and *HoxB2*, *HoxB3* and *HoxB4* are expressed below the 4 PA. *HoxB2*, *HoxB3* and *HoxB4* showed similar patterns of expression to those observe in mouse (Brend, 2003; Chan et al., 2010; Gavalas et al., 2001), with exception of *HoxB3* in the 3 PA. In this case, *HoxB3* expression is absent in the 3 PA of chicken embryo (figure 8C and 8I) as opposed to observed in mice (Chan et al., 2010). Interestingly, at both stages, *HoxB1* and *HoxB4* are specifically expressed in the posterior portion the 4 PP endoderm (Figure 7H and 7P), suggesting a possible role of these genes for positional identity of the pouches. However, mice without *HoxB4* showed deficiencies only in the specification of the ventral body wall (Manley et al., 2001) while the role of *HoxB1* is yet to be determined. However, *HoxB1* involvement in positive auto- and cross-regulatory mechanisms with other Hox genes and signalling factors (like retinoic acid) at the hindbrain level, has demonstrated the importance of these mechanisms to maintain a correct A-P expression pattern and how small disruptions in these domains alter the normal development of the different PA and PP (Gavalas *et al.*, 2001; Manzanares *et al*., 2001). Specifically, it has been demonstrated that an ectopic and anterior shift of *HoxB1* expression disrupts the normal development of the most anterior pouches (Mark *et al.*, 2004; Roberts *et al.*, 2006).

Together, the evidence from our results of *HoxA3* and *HoxB1* expression pattern in the 3/4 PP and previous studies in mice and chick, suggest *HoxA3*$^{+}$*HoxB1*$^{-}$ as the possible Hox-code responsible for the positional identity of the thymus in these pouches.

To further pursue our investigation to define the Hox-domains in the territory of the pouches we will study the domains of expression of others factors and signalling molecules known to be important for the formation of this organ (Rodewald, 2008; Gordon & Manley, 2011). For that, is one of our future goals to perform whole-mount *in situ* hybridization of these and other genes in isolated endoderm of 3/4PP of chick and quail at E3 and E4. This procedure was developed by our group (Neves *et al.*, 2012) and I had practiced it along this project. Isolation of 3D-preserved endoderm has been a challenging technique, so this is an on-going work.

V.2. Genetic manipulation of the Hox-code

To test our hypothesis of a possible Hox-code responsible for the positional identity of the thymus we designed a functional assay to evaluate the formation of this organ (section III.3, Le Douarin & Jotereau, 1975).

To genetically modify the endoderm to overexpress *HoxA3* and *HoxB1* we intend to use the combined system of vectors, *Tet-off* system of the combined system of vectors “Tol2-mediated gene transfer” and “Tetracycline-dependent conditional expression” (Sato *et al.*, 2007). In this project we constructed the pT2K-HoxA3eGFP recombinant plasmid (see Figure 11) and we are currently producing the pT2K-HoxB1eGFP construct. Future functional assays are required to test the construct pT2K-HoxA3eGFP.

Our final goal is to overexpress *HoxA3* in the 2 PP and test for the 2 PP to the 3 PP homeotic transformation with "gain-of-potential" of 2 PP to develop a thymus (and/or consequently the parathyroid glands). Also, we wanted to demonstrate the alternative situation, the "loss-of-potential" of the 3/4 PP to develop a thymus by overexpressing *HoxB1* in the 3 PP. In this case, we expected *HoxB1* to block the development of the thymus and/or the parathyroid glands. To test our hypothesis of a possible Hox-code responsible for the positional identity of the thymus we designed a functional assay to evaluate the formation of this organ (section III.2).

V.3. *In vitro* modulation of HEK 293T by the "Tol2-mediated gene transfer" and "Tetracycline-dependent conditional expression" combined system of vectors.

In order to study the efficiency of the combined system of vectors we transfected the human cell line, HEK 293T.

We started to test the more convenient plasmid concentration for an efficient transfection and capacity of genomic integration of these vectors. No significant differences were observed when using two different plasmid concentrations (Figure 10) and the integration capacity of these vectors in this genome was surprisingly low. This last result raises an important question about the possible low efficiency of this system when used *in vivo*. However, recent work from our group demonstrated that GFP expression is maintained in the neural tube after 12 days of *in ovo* electroporation showing the suitability of this system for *in vivo* studies.

Finally, we studied the modulation of system of vectors by doxycycline administration. Against our expectations, the time-course experiment showed a low level of GFP-expression when doxy is present in the culture. This event was previously reported when using the same cell line with the *Tet-on* system (Iguchi *et al*., 2012). In our *Tet-off system*, although GFP expression was detected in the presence of doxy, microscopic observation and flow cytometry analysis showed a significant decrease in GFP expression (and MFI) during the long-term culture, when compared with the condition with doxy removal (condition 1, figure 13 and figure 14). Also, when compared with transfected cultures grown without doxy (figure 11), the MFI of GFP^+ cells in doxy-conditions is significantly lower.

These evidences suggest the "GFP-expression leakage" observed in transfected cells grown in the presence of doxy is most likely related to a basal activity of the TRE promoter and not to an insufficient dose of doxy administration.

V.4. Technical considerations regarding the in situ hybridization procedures

We also experienced some problems with the whole-mount *in situ* hybridization and post-hybridization sectioning technique. Both in figure 7 and 8, for all probes except the new HoxA3 probe, we observe a more faintly expression of these genes in the post-hybridization sections

that are not comparable to the expression observed in the whole-mount hybridized embryos. The explanation encountered for this occurrence was the time and type of process when including the hybridized embryos in paraffin, before sectioning. Also, the problem observed in the sections of post-hybridized embryos for *HoxA3*, when using the new probe (Figure 7F and 7N), is the hybridization limited to the most exterior region of the embryos. This occurrence could be explained by an insufficient proteinase K treatment, which might not have permeabilize the embryo completely. Both technique and processing for sectioning need to be improved and standardized to a better result for these and in future gene expression pattern studies, as we may be losing important information on the domains of expression at tissue level.

VI. Final considerations and future perspectives

In this work, we were able to demonstrate, by whole-mount *in situ* hybridizations, that the endoderm of 3/4 PP, embryonic origin of the thymus and the parathyroid glands, are defined by the expression of HoxA3 and HoxB1 at E3 and E4, stages prior to the development of these organs. Therefore, and considering previous observations (Mark *et al.*, 2004; Roberts *et al.*, 2006), we hypothesized that the possible Hox-code responsible for the positional identity of the thymus would be defined by *HoxA3*$^{+}$*HoxB1*$^{-}$.

Moreover, we also characterized the expression pattern of different Hox genes along the A-P axis and, specifically, in the pharyngeal region, by whole-mount *in situ* hybridizations. This thorough characterization made possible the observation of Hox genes defining and possibly giving the identity to specific pouches of the chick embryo and demonstrated that the genes of the HoxB group studied were not following the general idea of an A-P expression patterning associated to Hox genes.

To further investigate and define the Hox-domains in the territory of the pouches we intend to perform whole-mount *in situ* hybridization of *HoxA3*, *HoxB1* and other thymus-related genes in isolated endoderms of 3/4 PP of chick and quail at E3 and E4.

Regarding the second aim of this project it was our intention to perform a functional assay for the manipulation of this putative Hox-code, *HoxA3*$^{+}$*HoxB1*$^{-}$, in the 2 PP and 3/4 PP and evaluate potential thymus development. We already produce one of the recombinant plasmids to be used in this assay, the pT2k-HoxA3eGFP and we are currently producing the pT2k-HoxB1eGFP. Both constructs will be integrated in the *Tet-off* combined system of vectors, which was evaluated *in vitro* during this project.

With this project we wish to unravel a little bit more of the gene network upstream to the development of the thymus and for the first time demonstrate *HoxA3* and *HoxB1* as the Hox-code with the capacity to define the positional identity of the thymus in the 3/4 PP, in avian embryos.

VII. References

Alves, N. L., Huntington, N. D., Rodewald, H.-R., & Di Santo, J. P. (2009). Thymic epithelial cells: the multi-tasking framework of the T cell "cradle". *Trends in immunology*, *30*(10), 468–74. doi:10.1016/j.it.2009.07.010

Barak, H., Preger-Ben Noon, E., & Reshef, R. (2012). Comparative spatiotemporal analysis of Hox gene expression in early stages of intermediate mesoderm formation. *Developmental dynamics : an official publication of the American Association of Anatomists*, *241*(10), 1637–49. doi:10.1002/dvdy.23853

Bel-Vialar, S., Itasaki, N., & Krumlauf, R. (2002). Initiating Hox gene expression: in the early chick neural tube differential sensitivity to FGF and RA signaling subdivides the HoxB genes in two distinct groups. *Development (Cambridge, England)*, *129*(22), 5103–15. Retrieved from http://www.ncbi.nlm.nih.gov/pubmed/12399303

Blackburn, C C, Augustine, C. L., Li, R., Harvey, R. P., Malin, M. a, Boyd, R. L., … Morahan, G. (1996). The nu gene acts cell-autonomously and is required for differentiation of thymic epithelial progenitors. *Proceedings of the National Academy of Sciences of the United States of America*, *93*(12), 5742–6. Retrieved from http://www.pubmedcentral.nih.gov/articlerender.fcgi?artid=39131&tool=pmcentrez&rendertype=abstract

Blackburn, C Clare, & Manley, N. R. (2004). Developing a new paradigm for thymus organogenesis. *Nature reviews. Immunology*, *4*(4), 278–89. doi:10.1038/nri1331

Bleul, C. C., Corbeaux, T., Reuter, A., Fisch, P., Mönting, J. S., & Boehm, T. (2006). Formation of a functional thymus initiated by a postnatal epithelial progenitor cell. *Nature*, *441*(7096), 992–6. doi:10.1038/nature04850

Bothe, I., Tenin, G., Oseni, A., & Dietrich, S. (2011). Dynamic control of head mesoderm patterning. *Development (Cambridge, England)*, *138*(13), 2807–21. doi:10.1242/dev.062737

Brend, T. (2003). Multiple levels of transcriptional and post-transcriptional regulation are required to define the domain of Hoxb4 expression. *Development*, *130*(12), 2717–2728. doi:10.1242/dev.00471

Capecchi, M. R. (1997). Hox genes and mammalian development. *Cold Spring Harbor symposia on quantitative biology*, *62*, 273–81. Retrieved from http://www.ncbi.nlm.nih.gov/pubmed/9598361

Chan, K. T., Qi, J., & Sham, M. H. (2010). Multiple coding and non-coding RNAs in the Hoxb3 locus and their spatial expression patterns during mouse embryogenesis. *Biochemical and biophysical research communications*, *398*(2), 153–9. doi:10.1016/j.bbrc.2010.05.150

Chisaka, O., & Capecchi, M. (1991). mouse homeobox gene hox-1.5. *Nature*. Retrieved from http://img.dxycdn.com/cms/upload/userfiles/file/2011/09/27/1316741389.pdf

Cordier, A. C., & Haumont, S. M. (1980). Development of thymus, parathyroids, and ultimobranchial bodies in NMRI and nude mice. *The American journal of anatomy*, *157*(3), 227–63. doi:10.1002/aja.1001570303

Couly, G., Creuzet, S., Bennaceur, S., Vincent, C., & Le Douarin, N. M. (2002). Interactions between Hox-negative cephalic neural crest cells and the foregut endoderm in patterning the facial skeleton in the vertebrate head. *Development (Cambridge, England)*, *129*(4), 1061–73. Retrieved from http://www.ncbi.nlm.nih.gov/pubmed/11861488

Creuzet, S., Couly, G., Vincent, C., & Le Douarin, N. M. (2002). Negative effect of Hox gene expression on the development of the neural crest-derived facial skeleton. *Development (Cambridge, England)*, *129*(18), 4301–13. Retrieved from http://www.ncbi.nlm.nih.gov/pubmed/12183382

De Robertis, E. M. (2008). The molecular ancestry of segmentation mechanisms. *Proceedings of the National Academy of Sciences of the United States of America*, *105*(43), 16411–2. doi:10.1073/pnas.0808774105

Douarin, NM Le, & Jotereau, F. (1975). Tracing of cells of the avian thymus through embryonic life in interspecific chimeras. *The Journal of experimental medicine*, *142*. Retrieved from http://jem.rupress.org/content/142/1/17.abstract

Duboule, D., & Dollé, P. (1989). The structural and functional organization of the murine HOX gene family resembles that of Drosophila homeotic genes. *The EMBO journal*, *8*(5), 1497–505. Retrieved from http://www.pubmedcentral.nih.gov/articlerender.fcgi?artid=400980&tool=pmcentrez&rendertype=abstract

Farley, A. M., Morris, L. X., Vroegindeweij, E., Depreter, M. L. G., Vaidya, H., Stenhouse, F. H., … Blackburn, C. C. (2013). Dynamics of thymus organogenesis and colonization in early human development. *Development (Cambridge, England)*, *140*(9), 2015–26. doi:10.1242/dev.087320

Gavalas, A., Trainor, P., Ariza-McNaughton, L., & Krumlauf, R. (2001). Synergy between Hoxa1 and Hoxb1: the relationship between arch patterning and the generation of cranial neural crest. *Development*, *128*(15), 3017–3027. Retrieved from http://dev.biologists.org/content/128/15/3017.long

Gordon, J, Bennett, a R., Blackburn, C. C., & Manley, N. R. (2001). Gcm2 and Foxn1 mark early parathyroid- and thymus-specific domains in the developing third pharyngeal pouch. *Mechanisms of development*, *103*(1-2), 141–3. Retrieved from http://www.ncbi.nlm.nih.gov/pubmed/11335122

Gordon, Julie, & Manley, N. R. (2011). Mechanisms of thymus organogenesis and morphogenesis. *Development (Cambridge, England)*, *138*(18), 3865–78. doi:10.1242/dev.059998

Graham, a, & Smith, A. (2001). Patterning the pharyngeal arches. *BioEssays : news and reviews in molecular, cellular and developmental biology*, *23*(1), 54–61. doi:10.1002/1521-1878(200101)23:1<54::AID-BIES1007>3.0.CO;2-5

Graham, A. (2001). The development and evolution of the pharyngeal arches. *Journal of anatomy*, *199*(Pt 1-2), 133–41. Retrieved from http://www.pubmedcentral.nih.gov/articlerender.fcgi?artid=1594982&tool=pmcentrez&rendertype=abstract

Graham, Anthony, & Richardson, J. (2012). Developmental and evolutionary origins of the pharyngeal apparatus. *EvoDevo*, *3*(1), 24. doi:10.1186/2041-9139-3-24

Grevellec, A., & Tucker, A. S. (2010). The pharyngeal pouches and clefts: Development, evolution, structure and derivatives. *Seminars in cell & developmental biology*, *21*(3), 325–32. doi:10.1016/j.semcdb.2010.01.022

Günther, T., Chen, Z. F., Kim, J., Priemel, M., Rueger, J. M., Amling, M., … Karsenty, G. (2000). Genetic ablation of parathyroid glands reveals another source of parathyroid hormone. *Nature*, *406*(6792), 199–203. doi:10.1038/35018111

Hamburger, V., & Hamilton, H. (1951). A series of normal stages in the development of the chick embryo. *Journal of morphology*, *88*(1). Retrieved from http://homepage.univie.ac.at/~metschb9/Hamburger51_ChickStages.pdf

Holland, P. W. H. (2013). Evolution of homeobox genes. *Wiley interdisciplinary reviews. Developmental biology*, *2*(1), 31–45. doi:10.1002/wdev.78

Holland, P. W. H., & Takahashi, T. (2005). The evolution of homeobox genes: Implications for the study of brain development. *Brain research bulletin*, *66*(4-6), 484–90. doi:10.1016/j.brainresbull.2005.06.003

Hunt, P., & Krumlauf, R. (1991). Deciphering the Hox code: clues to patterning branchial regions of the head. *Cell*, *66*(6), 1075–8. Retrieved from http://www.ncbi.nlm.nih.gov/pubmed/1680562

Hunt, P., & Krumlauf, R. (1992). Hox codes and positional specification in vertebrate embryonic axes. *Annual review of cell biology*, *8*, 227–56. doi:10.1146/annurev.cb.08.110192.001303

Iguchi, T., Yagi, H., Wang, C.-C., & Sato, M. (2012). A tightly controlled conditional knockdown system using the Tol2 transposon-mediated technique. *PloS one*, *7*(3), e33380. doi:10.1371/journal.pone.0033380

Krumlauf, R. (1994). Hox genes in vertebrate development. *Cell*, *78*(2), 191–201. Retrieved from http://www.sciencedirect.com/science/article/pii/0092867494902909

Le Douarin, N. (1967). [Influence of the nature and the degree of evolution of the mesoderm on differentiation of pharyngeal endoderm in the chick embryo]. *Comptes rendus des séances de la Société de biologie et de ses filiales*, *161*(2), 431–4. Retrieved from http://www.ncbi.nlm.nih.gov/pubmed/4229156

Liu, G., Moro, A., Zhang, J. J. R., Cheng, W., Qiu, W., & Kim, P. C. W. (2007). The role of Shh transcription activator Gli2 in chick cloacal development. *Developmental biology*, *303*(2), 448–60. doi:10.1016/j.ydbio.2006.10.051

Manley, N R, Barrow, J. R., Zhang, T., & Capecchi, M. R. (2001). Hoxb2 and hoxb4 act together to specify ventral body wall formation. *Developmental biology*, *237*(1), 130–44. doi:10.1006/dbio.2001.0365

Manley, N R, & Capecchi, M. R. (1995). The role of Hoxa-3 in mouse thymus and thyroid development. *Development (Cambridge, England)*, *121*(7), 1989–2003. Retrieved from http://www.ncbi.nlm.nih.gov/pubmed/7635047

Manley, N R, & Capecchi, M. R. (1998). Hox group 3 paralogs regulate the development and migration of the thymus, thyroid, and parathyroid glands. *Developmental biology*, *195*(1), 1–15. doi:10.1006/dbio.1997.8827

Manley, Nancy R, & Condie, B. G. (2010). Transcriptional regulation of thymus organogenesis and thymic epithelial cell differentiation. *Progress in molecular biology and translational science*, *92*, 103–20. doi:10.1016/S1877-1173(10)92005-X

Manzanares, M., Bel-Vialar, S., Ariza-McNaughton, L., Ferretti, E., Marshall, H., Maconochie, M. M., … Krumlauf, R. (2001). Independent regulation of initiation and maintenance phases of Hoxa3 expression in the vertebrate hindbrain involve auto- and cross-regulatory mechanisms. *Development (Cambridge, England)*, *128*(18), 3595–607. Retrieved from http://www.ncbi.nlm.nih.gov/pubmed/11566863

Mark, M., Ghyselinck, N. B., & Chambon, P. (2004). Retinoic acid signalling in the development of branchial arches. *Current opinion in genetics & development*, *14*(5), 591–8. doi:10.1016/j.gde.2004.07.012

McGinnis, W., & Krumlauf, R. (1992). Homeobox genes and axial patterning. *Cell*, *68*(2), 283–302. Retrieved from http://www.ncbi.nlm.nih.gov/pubmed/1346368

Nehls, M., Kyewski, B., Messerle, M., Waldschutz, R., Schuddekopf, K., Smith, a. J. H., & Boehm, T. (1996). Two Genetically Separable Steps in the Differentiation of Thymic Epithelium. *Science*, *272*(5263), 886–889. doi:10.1126/science.272.5263.886

Neves, H., Dupin, E., Parreira, L., & Le Douarin, N. M. (2012). Modulation of Bmp4 signalling in the epithelial-mesenchymal interactions that take place in early thymus and parathyroid development in avian embryos. *Developmental biology*, *361*(2), 208–19. doi:10.1016/j.ydbio.2011.10.022

Prince, V., & Lumsden, a. (1994). Hoxa-2 expression in normal and transposed rhombomeres: independent regulation in the neural tube and neural crest. *Development (Cambridge, England)*, *120*(4), 911–23. Retrieved from http://www.ncbi.nlm.nih.gov/pubmed/7600967

Robertis, E. De. (2008). Evo-devo: variations on ancestral themes. *Cell*, *132*(2), 185–195. Retrieved from http://www.sciencedirect.com/science/article/pii/S0092867408000500

Roberts, C., Ivins, S., Cook, A. C., Baldini, A., & Scambler, P. J. (2006). Cyp26 genes a1, b1 and c1 are down-regulated in Tbx1 null mice and inhibition of Cyp26 enzyme function produces a phenocopy of DiGeorge Syndrome in the chick. *Human molecular genetics*, *15*(23), 3394–410. doi:10.1093/hmg/ddl416

Roberts, D. J., Johnson, R. L., Burke, a C., Nelson, C. E., Morgan, B. a, & Tabin, C. (1995). Sonic hedgehog is an endodermal signal inducing Bmp-4 and Hox genes during induction and regionalization of the chick hindgut. *Development (Cambridge, England)*, *121*(10), 3163–74. Retrieved from http://www.ncbi.nlm.nih.gov/pubmed/7588051

Rodewald, H.-R. (2008). Thymus organogenesis. *Annual Review of Immunology*, *26*, 355–88. doi:10.1146/annurev.immunol.26.021607.090408

Santagati, F., Minoux, M., Ren, S.-Y., & Rijli, F. M. (2005). Temporal requirement of Hoxa2 in cranial neural crest skeletal morphogenesis. *Development (Cambridge, England)*, *132*(22), 4927–36. doi:10.1242/dev.02078

Santos, M. A., Sarmento, L. M., Rebelo, M., Doce, A. A., Maillard, I., Dumortier, A., … Demengeot, J. (2007). Notch1 engagement by Delta-like-1 promotes differentiation of B lymphocytes to antibody-secreting cells. *Proceedings of the National Academy of Sciences of the United States of America*, *104*(39), 15454–9. doi:10.1073/pnas.0702891104

Sato, Y., Kasai, T., Nakagawa, S., Tanabe, K., Watanabe, T., Kawakami, K., & Takahashi, Y. (2007). Stable integration and conditional expression of electroporated transgenes in chicken embryos. *Developmental biology*, *305*(2), 616–24. doi:10.1016/j.ydbio.2007.01.043

Scott, M. P. (1992). Vertebrate homeobox gene nomenclature. *Cell*, *71*(4), 551–553. doi:10.1016/0092-8674(92)90588-4

Veitch, E., Begbie, J., Schilling, T. F., Smith, M. M., & Graham, A. (1999). Pharyngeal arch patterning in the absence of neural crest. *Current biology : CB*, *9*(24), 1481–1484. Retrieved from http://www.ncbi.nlm.nih.gov/pubmed/10607595

Watanabe, T., Saito, D., Tanabe, K., Suetsugu, R., Nakaya, Y., Nakagawa, S., & Takahashi, Y. (2007). Tet-on inducible system combined with in ovo electroporation dissects multiple roles of genes in somitogenesis of chicken embryos. *Developmental biology*, *305*(2), 625–36. doi:10.1016/j.ydbio.2007.01.042

Watari-Goshima, N., & Chisaka, O. (2011). Chicken HOXA3 gene: its expression pattern and role in branchial nerve precursor cell migration. *International journal of biological sciences*, *7*(1), 87–101. Retrieved from http://www.pubmedcentral.nih.gov/articlerender.fcgi?artid=3030145&tool=pmcentrez&rendertype=abstract

Wilkinson, D. G. (1989). Homeobox genes and development of the vertebrate CNS. *BioEssays : news and reviews in molecular, cellular and developmental biology*, *10*(2-3), 82–5. doi:10.1002/bies.950100211

Zenatti, P. P., Ribeiro, D., Li, W., Zuurbier, L., Silva, M. C., Paganin, M., … Barata, J. T. (2011). Oncogenic IL7R gain-of-function mutations in childhood T-cell acute lymphoblastic leukemia. *Nature genetics*, *43*(10), 932–9. doi:10.1038/ng.924

APPENDIX I– BUFFERS, MEDIA AND OTHER SOLUTIONS

Buffers for multiple uses

1x TAE

EDTA (pH=8)	1 mM
Acetic acid	20 mM
Tris base	40 mM

1x PBS

NaCl	137 mM
KCL	2.7 mM
Na2HPO4	10 mM
KH2PO4	2 mM

Adjust pH to 7.4 with HCl

PBT 0.1%

Triton	0.1%
PBS 1x	To final volume

Bacterial growth media

Lysogeny Broth (LB) medium

Tryptone	1%
Yeast extract	0.5%
NaCl	1%

Lysogeny Broth (LB) agar

7.5 g agar per 500 mL of LB medium

Whole mount *in situ* hybridization' solutions

3.7% Paraformaldehyde (PFA) in PBS

7.4% PFA (stock)	1:2
PBS 1x	1:2

PBT 0.1%

Triton	0.1%
PBS 1x	To final volume

Hybridization Solution	**Stock Solution**	**100 mL**
50% Formamide	100%	50 mL
1.3X SSC pH=5	20X	7.5 mL
5 mM EDTA pH=8	500 mM	1 mL
50 µg/ml Yeast RNA	20 mg/mL	250 µL

0.2% Tween 20	100%	0.4 mL
0.5% CHAPS	10%	5 mL
100 µg/mL Heparine	50 mg/mL	0.2 mL
H2O		35.65 mL

MAB pH=7,5	**Stock Solution**	**100 mL**
0.1 M Maleic Acid	2 M	5 mL
0.15 M NaCl	5 M	3 mL
NaOH	10 N	1.5+0.5 mL
H2O		90 mL

Adjust pH to 7.5 with NaOH 10N

MABT: 0.1% Tween 20/MAB

NTM pH=9.5	**Stock Solution**	**100 mL**
0.1 M Tris pH=9.5	1 M	10 mL
0.1 M NaCl	5 M	2 mL
MgCl2	2 M	2.5 mL
H2O		85.5 mL

Washing solution

100% Formamide	50%
20x SSC pH=7.5	1x
Tween 20	0.1%
H2O	To final volume

APPENDIX II - RIBOPROBES AND PROTOCOLS

Riboprobes

Table 1 | Restriction enzymes and RNA Polymerases used to generate different Hox genes sense and antisense riboprobes.

Probe	Vector	Antisense	Sense	RNA polymerase	Origin
HoxA2	pGEM-T easy	HindIII	ND	T3	S. Creuzet
HoxA3	pGEM-T easy	BamHI	ND	T7	S. Creuzet
HoxA3	TOPO II PCR	SpeI	EcoRV	T7 (antisense) / SP6 (sense)	This study
HoxB1	pGEM-T easy	PstI	ND	T7	Alev *et al.* 2010
HoxB2	pGEM-T easy	SpeI	EcoRV	T7 (antisense) / SP6 (sense)	This study
HoxB3	pGEM-T easy	SalI	ND	T7	Alev *et al.* 2010
HoxB4	pGEM-T	SpeI	EcoRV	T7 (antisense) / SP6 (sense)	This study

ND, not developed

Protocols

Preparation and transformation of competent DH5α strain of *E.coli*

Non-competent bacterial cells from frozen glycerol stock were streak out onto LB plate and grown o/n. Single colonies were selected for the starter culture with 3 mL of fresh LB without antibiotics and grown o/n in a 37°C shaker (225 rpm).The next day 2 mL from the starter culture were diluted into 200 mL of fresh LB without antibiotics and incubated in a 37°C shaker (225 rpm) for 3 h (until it reaches optical density at 600 nm (OD600) of 0.4–0.6). The culture was collected and put on ice (it is important to keep the cells and solutions on ice for the rest of the protocol). The cells were harvested at 4000 rpm for 5 min at 4°C and the supernatant removed. After adding half of the initial volume of cold MgCl2 0.1 M, cells were harvested again and the supernatant removed again. Afterwards, it was added half of the initial volume of cold CaCl2 0.1 M and incubated on ice for 30 min. The cells were harvested again, the supernatant removed, and the pellet was resuspended in CaCl2 0.1 M/15% Glycerol to 1/15 of the original/initial volume. The final volume suspension was distributed in aliquots of 500 µL into 1.5 mL criotubes and stored at -80°C.

To transform DH5α cells, between 1-10 µL (15-20 µL from ligations) of circular plasmid DNA were incubated with 100-200 µL of competent bacteria (DH5α) for 20 min on ice. Then, they were exposed to a heat shock at 42ºC for 2 min followed by cooling on ice for 10 min. Next, 1 mL of LB medium was added and incubated in a 37°C shaker (225 rpm) for 45 min. Bacteria were plated (20-300 µL) on solid LB Agar medium containing ampicillin (100 µg/mL) (Sigma) and incubated o/n at 37°C to select the transformed bacteria.

Phenol:Chloroform extraction and precipitation with ethanol

This step was performed to remove proteins from a nucleic acid solution. It was added 150 µL of phenol:chloroform 1:1 (v/v) (Ambion) per sample and the lower phase (chloroform) was removed by pipetting with thin tips. After centrifuging at 11000 rpm for 5 min at 4°C, the lower

phase was removed again. Then, 150 µL of chloroform was added per sample, centrifuged at 11000 rpm for 10 min at 4°C and the lower phase removed. The aqueous phase, which contains nucleic acids, is the one that remains and 15 µL of sodium acetate (NaAC) 3 M and 450 µL of absolute ethanol were added per sample. After the precipitation of the DNA by incubating at -80°C for 30 min, the mixture was centrifuged at 13000 rpm for 30 min at 4°C. The supernatant was removed and the pellet dried and resuspended in 10 µL of RNase-free water.

Whole-mount *in situ* hybridization

1. Dissect embryos in PBS and remove as much of the extra-embryonic membranes as possible.
2. Fix the embryos in 3.7% Paraformaldehyde/PBS, leave in the roller for some time at room temperature and keep/store at 4°C o/n.
3. Wash two times in PBT (0.1% Tween-20/PBS) for 5 min (Roller).
4. Dehydration:
   4.1. Wash embryos in 50% Methanol/PBT for 5 min (Roller).
   4.2. Wash two times in 100% Methanol (Roller) for 5 min and store at -20°C o/n. (it can be stored up to one month). This o.n. incubation can be replaced by an incubation at -80°C for 1-2h.
5. Rehydrate embryos through Methanol series: 75%, 50%, 25% Methanol/PBT (Roller) for 5 min each.
6. Wash two times in PBT (Roller).
7. Permeabilize embryos with 20 µg/mL proteinase K in PBT (Roller) (1h30 and 2h for E3 and E4 embryos, respectively).
8. Transfer the permeabilized embryos directly to Post-Fixation solution: 3.7% Paraformaldehyde /0.1% Glutaraldehyde/PBT, for 20 min.
9. Rinse and wash once with PBT for 5 min (Roller).
10. Transfer the embryos to a proper/suitable hybridization tube.

Hybridization:

11. Rinse once with 1:1 hybridization solution/PBT mix; rinse with 2 mL of new hybridization solution/PBT and let embryos settle.
12. Rinse with hybridization solution. Rinse with 2 mL of new hybridization solution and let embryos settle.
13. Replace with 1 mL hybridization solution and prehybridize at 70°C for 2 h.
14. Replace the hybridization solution by 1 mL of pre-warmed hybridization solution with ≈400ng/mL of DIG-labeled RNA probe and hybridize at 70°C o/n.

Post-Hybridization washes:

15. Rinse twice with prewarmed (70°C) hybridization solution.
16. Wash twice with prewarmed (70°C) hybridization solution for 40 min.
17. Wash with prewarmed (70°C) hybridization solution: Maleic Acid Buffer (MABT) for 30 min.

18. Rinse twice with MABT.
19. Wash twice with MABT for 30 min. (Roller)

Imuno

20. Block with 2% Boehringer Blocking Solution (BBS)/20% heat treated Fetal Bovine Serum (FBS)/MABT for 2 h (Roller).
21. Incubate with 1:2000 Anti-Digoxigenin-AP, Fab fragments antibody (Roche) in 2% BBS/20% FBS/MABT o/n.

Post-antibody washes and Revelation

22. Rinse 3 times with MABT (Roller) for 1-2 h. In the second rinse, perforate cephalic vesicles of the embryos and transfer them to larger tubes.
23. Wash with MABT for 2-3 days with a 12 h frequency (Roller).
24. Wash twice with NTM for 10 min.
25. Reveal with 0.45µL NBT (nitro blue tetrazolium chloride) + 3,5µL BCIP (5-bromo-4-chloro-3-indolyl-phosphate) in 1 mL NTM. Incubate at 37°C protected from light. Follow regularly the revelation reaction.
26. When color has developed to the desired extent, stop reaction by washing 3 times with PBT. Replace the PBT for PBS and store at 4°C until acquisition of pictures. Store indefinitely in 3.7% PFA/PBS at 4°C.

HEK 293T and murine 3T3 cell lines tranfection protocol

For the transfection of the HEK 293T and 3T3 cell lines, we used a standard calcium phosphate-mediated transfection protocol for mammalian cell lines was used, in which the vector in the form of plasmid DNA is mixed with calcium chloride ($CaCl_2$) and HEPES-buffered saline solution (HBSS, Sigma) to form a transfection mix precipitate to be taken up by the cells (Swift *et al.*, 1999). When cells reached 30-40% of confluence, we trypsinized and count them. 0.3 to 0.5M cells were resuspended in 2 mL of maintenance medium and plated per well in a 6-well plate (each well representing a transfection condition) and grown o/n till they reached 30-40% of confluence. 1h before transfection, medium was changed and 0.25µM Chloroquine was added due to its lysosomal neutralizing activity. In conditions where doxycycline is to be present, 1 and 5 µg of this antibiotic were also added at this time. Transfection mix was added gently, dropwise, to each condition and the cells were left o/n in the incubator. At 24h post-transfection medium is changed to new fresh medium and supplemented with 20 mM Hepes.